The Journal of Comparative Neurology 513:622–642 (2009)

Cortical Connections of the Visuomotor Parietooccipital Area V6Ad of the Macaque Monkey

MICHELA GAMBERINI,[1] LAURETTA PASSARELLI,[1] PATRIZIA FATTORI,[1] MINO ZUCCHELLI,[2] SOPHIA BAKOLA,[1,3] GIUSEPPE LUPPINO,[4] AND CLAUDIO GALLETTI[1]*

[1]Dipartimento di Fisiologia Umana e Generale, Università di Bologna, I-40127 Bologna, Italy
[2]Divisione di Neurochirurgia, Dipartimento di Neuroscienze, Ospedale Bellaria di Bologna, I-40100 Bologna, Italy
[3]Department of Basic Sciences, School of Health Sciences, University of Crete, GR-71003 Iraklion, Greece
[4]Dipartimento di Neuroscienze, Sezione di Fisiologia, Università di Parma, I-43100 Parma, Italy

ABSTRACT

Area V6A, a functionally defined region in the anterior bank of the parietooccipital sulcus, has been subdivided into dorsal and ventral cytoarchitectonic fields (V6Ad and V6Av). The aim of this study was to define the cortical connections of the cytoarchitectonic field V6Ad. Retrograde and bidirectional neuronal tracers were injected into the dorsal part of the anterior bank of parietooccipital sulcus of seven macaque monkeys (*Macaca fascicularis*). The limits of injection sites were compared with those of cytoarchitectonic fields. The major connections of V6Ad were with areas of the superior parietal lobule. The densest labeling was observed in the medial intraparietal area (MIP). Areas PEc, PGm, and V6Av were also strongly connected. Labeled cells were found in medial parietal area 31; in cingulate area 23; in the anterior (AIP), ventral (VIP), and lateral (LIP) intraparietal areas; in the inferior parietal lobule (fields Opt and PG); and in the medial superior temporal area (MST). In the frontal lobe, the main projection originated from F2, although labeled cells were also found in F7 and area 46. Preliminary results obtained from injections in nearby areas PEc and V6Av revealed connections different from those of V6Ad. In agreement with functional data, the strong connections with areas where arm-reaching activity is represented suggest that V6Ad is part of a parietofrontal circuit involved in the control of prehension, and connections with AIP specifically support an involvement in the control of grasping. Connections with areas LIP and Opt are likely related to the oculomotor activities observed in V6Ad. J. Comp. Neurol. 513: 622–642, 2009. © 2009 Wiley-Liss, Inc.

Indexing terms: dorsal visual stream; posterior parietal cortex; cytoarchitecture; visuomotor integration; parietofrontal circuit

Functional studies in alert monkeys have revealed the existence of two visual areas in the caudalmost part of the macaque superior parietal lobule (SPL): V6 and V6A (Galletti et al., 1996; see Fig. 1). V6 is a classic, retinotopically organized, extrastriate area in which the representation of the periphery of visual field is relatively emphasized in comparison with other extrastriate areas (Galletti et al., 1999a). V6A is a visuomotor area containing visual, somatic, oculomotor, and reaching neurons as well as cells modulated by the level of animal's attention (Galletti et al., 1996, 1999b, 2003). In contrast with V6, area V6A is organized according to a coarse topographic order, with cells with receptive fields that include central vision tending to be located dorsal to those with receptive fields restricted to the far periphery (Galletti et al., 1999b). Both V6 and V6A overlap to some extent with the parietooccipital field (PO) recognized in earlier studies of the macaque cortex (Colby et al., 1988) and have likely homologues in other species of primate (Rosa and Tweedale, 2001; Galletti et al., 2005; Pitzalis et al., 2006).

Previous studies (Matelli et al., 1998; Shipp et al., 1998; Marconi et al., 2001) reported somewhat different patterns of cortical connections of the dorsal part of the anterior bank of the parietooccipital sulcus, putatively area V6A. The most striking difference regards the connections with the dorsal premotor frontal cortex. According to Matelli and collaborators (1998), V6A is connected mainly with F2, corresponding to area 6DC of Barbas and Pandya (1987). According to Shipp and coworkers (1998), V6A is connected mainly with F7, corresponding to area 6DR of Barbas and Pandya (1987). According to Marconi and coworkers (2001), V6A is connected with F7, but not with F2. One possible explanation for the discrep-

Grant sponsor: European Union; Grant number: FP6-IST-027574-MATHESIS; Grant sponsor: Ministero dell'Istruzione dell'Università e della Ricerca; Grant sponsor: Fondazione del Monte di Bologna e Ravenna.

*Correspondence to: Prof. Claudio Galletti, Dipartimento di Fisiologia Umana e Generale, Università di Bologna, I-40127 Bologna, Italy.
E-mail: claudio.galletti@unibo.it

Received 19 May 2008; Revised 17 October 2008; Accepted 16 December 2008

DOI 10.1002/cne.21980

Published online in Wiley InterScience (www.interscience.wiley.com).

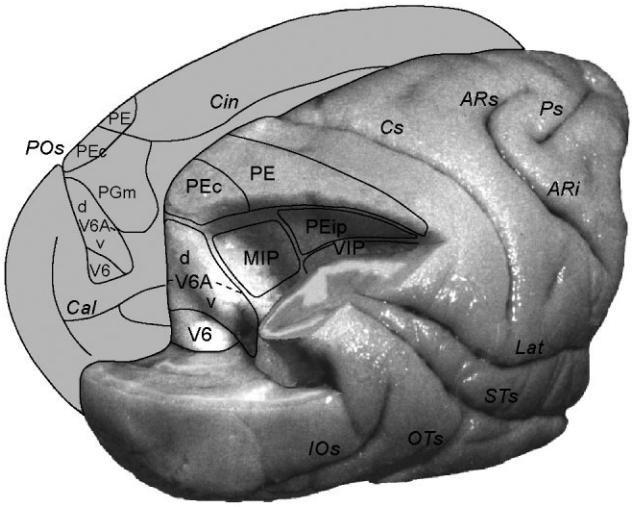

Figure 1.
Posterolateral view of a partially dissected macaque brain (modified from Galletti et al., 1996). The inferior parietal lobule of the right hemisphere has been cut away at the level of the fundus of the intraparietal sulcus to show the cortex of the medial bank of this sulcus. The occipital lobe of the same hemisphere has been cut away at the level of the fundus of the parietooccipital and lunate sulci to show the cortex of the anterior bank of the parietooccipital sulcus. The mesial surface of the left hemisphere is drawn, with the main sulci and the posterior parietal areas reported. POs, parietooccipital sulcus; Cal, calcarine sulcus; Cin, cingulate sulcus; IOs, inferior-occipital sulcus; OTs, occipitotemporal sulcus; STs, superior temporal sulcus; Lat, lateral sulcus; Cs, central sulcus; ARs, superior arcuate sulcus; ARi, inferior arcuate sulcus; Ps, principal sulcus; areas V6, V6Ad, V6Av, PEc, PE, MIP, PEip, VIP, PGm are also indicated.

ancy is that V6A is not a homogeneous cortical field. This hypothesis has already been advanced in the past to explain the dorsal/ventral segregation of some functional properties within V6A (Fattori et al., 1999; Galletti et al., 1999b) as well as the differential distribution of labeling observed following tracer injections in other cortical areas (Matelli et al., 1998; Galletti et al., 2001). A recent study has lent support to this hypothesis by showing multiple architectonic fields in the anterior bank of the parietooccipital sulcus (Luppino et al., 2005). In addition to a typical cytoarchitectonic field corresponding to the functionally defined area V6, this study found two cytoarchitectonic fields within the limits of area V6A: a ventral field, which has been named V6Av, and a dorsal field, named V6Ad (see Fig. 1; Luppino et al., 2005). V6Av is more representative of the visual domain and V6Ad of the somatomotor domain (Fattori et al., 1999), in particular the upper limbs (Fattori et al., 2001, 2004; Breveglieri et al., 2002). In the present study, we have traced the cortical connections of area V6Ad as a first step of a thorough study aimed to clarify in detail the connectivity patterns of the various anterior parietooccipital areas. Preliminary data have been previously presented in abstract form (Passarelli et al., 2007a,b).

MATERIALS AND METHODS

Seven male macaque monkeys (*Macaca fascicularis*, 3–7 kg) were used in this study. Tracer injections were placed in area V6Ad or in the neighboring areas V6Av and PEc as architectonically defined. Table 1 summarizes the locations of injections, the injected tracers, and their amount. Experimental protocols were approved by the Bioethical Committee of the University of Bologna and complied with the national and European laws on the care and use of laboratory animals.

TABLE 1. Injections Sites and Neuronal Tracers Employed in the Experiments

Case	Injection site	Tracer	Amount and concentration	Functional study
A1R	V6Ad	CTB red	1.5 μl, 1%	No
A2R	PEc	CTB green	1.5 μl, 1%	No
A3R	V6Ad	FB	0.2 μl, 3%	No
	PEc (V6Ad)	DY	0.2 μl, 2,5%	No
A3L	V6Ad	CTB red	1.5 μl, 1%	No
	V6Ad	CTB green	1.5 μl, 1%	No
11L	V6Ad	WGA-HRP	0.2+0.28 μl, 4%	No
17R	V6Av	CTB gold	0.8 μl, 0.5%	Yes
18L	V6Ad (V6Av)	WGA-HRP	0.08 μl, 4%	Yes
	V6Av (V6Ad)	CTB gold	0.8 μl, 0.5	Yes
19L	V6Ad (PEc)	FB	0.2 μl, 3%	Yes

Experimental procedures, tracer injections, and histological processing

In four animals (A1R, A2R, A3R, A3L, and 11L), the target region was directly visualized during surgery. The animals were anesthetized with ketamine hydrochloride (15 mg/kg i.m.), followed by i.v. injections of sodium thiopental. After craniotomy, the dura mater was retracted, and the parietooccipital sulcus was gently opened in order to expose the anterior bank. A glass micropipette attached to the syringe needle was moved on to enter directly into the anterior bank of the parietooccipital sulcus. The location of the injection site was chosen on the basis of anatomical landmarks, using the architectonic map of the anterior wall of the parietooccipital sulcus as frame of reference. After the injections, the dural flap was sutured, the bone was replaced, and the superficial tissues were sutured in layers. During surgery, hydration was maintained with saline (about 10 ml/hour, i.v.), and temperature was maintained with a heating pad. Heart rate, blood pressure, respiratory depth, and body temperature were continuously monitored. Upon recovery from anesthesia, the animals were returned to their home cages and closely monitored. Analgesics (ketorolac, 1 mg/kg, i.m.) and antibiotics (erythromycin, 1–1.5 ml/10 kg) were provided postoperatively.

In the remaining three animals used in the present study (17R, 18L, and 19L), which have been the subjects in chronic single-unit recording studies, the areas of the anterior wall of the parietooccipital sulcus were functionally identified before the tracing experiments. Details of training, animal care, and surgical and recording procedures, as well as the reconstruction of recording sites, are reported elsewhere (Galletti et al., 1995, 1999b, 2001, 2005). The following is a brief description of the procedures relevant for the purposes of the present study.

During recording sessions, the animals sat in a primate chair facing a large (80° × 80°) tangent screen. They performed a fixation task, with the head restrained, while glass-coated Elgiloy microelectrodes (Suzuki and Azuma, 1976) were advanced through the intact dura mater using a remote-controlled microdrive, which was fitted daily on a recording chamber fixed to the skull. Eye positions were recorded by an infrared oculometer (Bach et al., 1983). The sample rate for

action potentials was 1 kHz and that for eye position 100 Hz. Standard visual stimuli (different in form, color, size, orientation, and direction and speed of movement) were used for testing the visual responsiveness of cells in record and for mapping their visual receptive fields.

At the end of recording sessions, neural tracers were injected by using a "recording syringe" (i.e., a 1-μl Hamilton syringe with a metal microelectrode attached to the needle) in order to inject neuronal tracer into physiologically identified different parts of V6A. The needle of this syringe was advanced through the intact dura by the same remote-controlled microdrive used to advance the microelectrode.

The reconstruction of the recording syringe penetration in case 18L is shown in Figure 2. The needle of the syringe (and the electrode) traversed areas V1 and V2 before reaching the anterior bank of parietooccipital sulcus, where area V6A can be functionally recognized on the basis of the criteria previously described by Galletti and coworkers (1999b). Some V6A cells encountered along this penetration were activated by complex visual stimuli (light/dark gratings and corners of different orientation, direction and speed of movement, or visual stimuli continuously changed in order to avoid a rapid adaptation), one cell showed a real-position behavior (Galletti et al., 1993), and others appeared to be insensitive to visual stimulation. As shown in Figure 2, the receptive fields of V6A neurons were much larger than those of visual cells recorded from the occipital lobe and showed a large scatter, as typically observed in area V6A (Galletti et al., 1999b). Despite the interruptions caused by nonresponsive cells, a coarse topographic trend from near-peripheral (30–40°) to far-peripheral (up to 80°) existed as the electrode travelled ventrally in the anterior bank, in agreement with the previous results in V6A (Galletti et al., 1999b).

The fluorescent tracers Fast blue (FB; 3% in distilled water; EMS-Polyloy GmbH, Gross-Umstadt, Germany, and Polysciences Europe GmbH, Heidelberg, Germany), diamidino yellow (DY; 2.5% in phosphate buffer 0.2 M, pH 7.2; Sigma, St. Louis, MO), cholera toxin B subunit conjugated with Alexa fluor 488 (CTB green; 1% in PBS; Molecular Probes, Eugene, OR) or with Alexa fluor 594 (CTB red, 1% in PBS; Molecular Probes), cholera toxin B subunit conjugated with colloidal gold (CTB gold; 0.5% in distilled water; List, Campbell, CA), and wheat germ agglutinin conjugated with horseradish peroxidase (WGA-HRP; 4% in distilled water; Sigma) were slowly pressure injected through the glass micropipette (tip diameter 50–100 μm) attached to a 1-μl or 5-μl Hamilton microsyringe (Hamilton, Reno, NV), depending on the amount of the injected tracer.

In all cases, injections were carried out by releasing several small amounts of tracer around the center of the cortical depth. Each release was 0.02 or 0.2 μl depending of total amount of tracer to be injected and was made over a period of 2 minutes, with 5 minutes between releases. Typically, total injection time was about 30–40 minutes, with total injection volumes ranging from 0.08 to 1.5 μl. The needle was left in place for 25–30 minutes and then was withdrawn from the brain very slowly.

As described by Galletti et al. (2001), a series of measures was taken to minimize the leakage of tracer along the needle track. In case of tracer leakage (case 17R), the knowledge of retinotopic organization of areas V1 and V2 helped us in

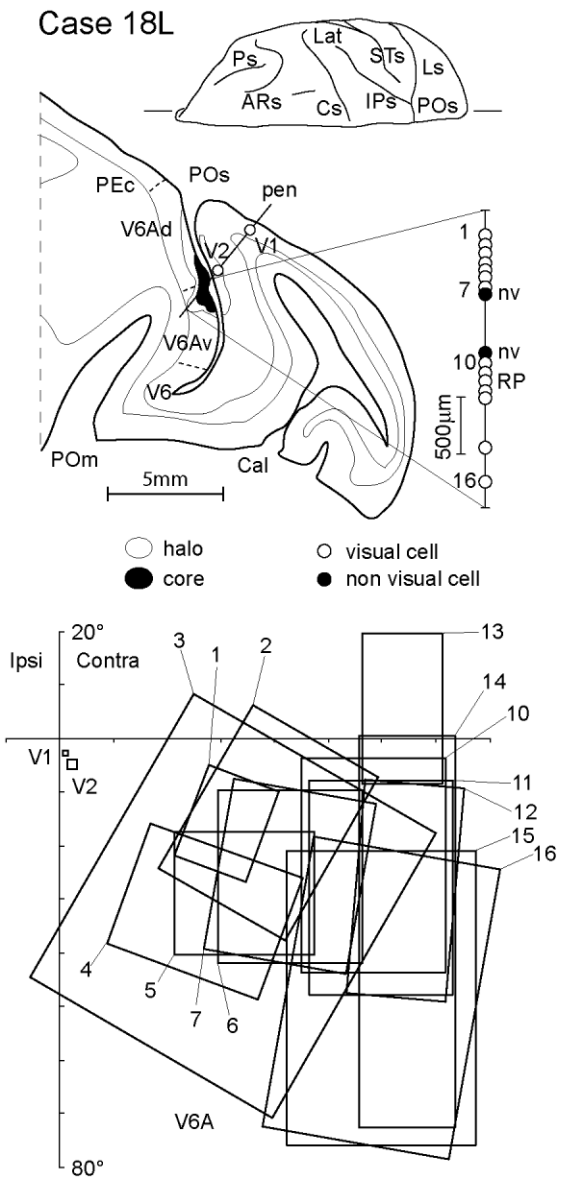

Figure 2.
Location of the injection site in case 18L and reconstruction of the penetration carried out with the recording syringe. **Top:** Parasagittal section of the brain containing the reconstruction of the penetration carried out with the recording syringe (pen). The section was taken at the level indicated on the brain silhouette on the top. Dashed lines on the section represent the cytoarchitectonic borders of the different sectors of area V6A (Luppino et al., 2005). "Halo" and "core" zones of injection site are reported on the section as white and black areas, respectively. Dots along the penetration represent locations of the cells isolated in areas V1 and V2. The recording sites in area V6Ad/V6Av are represented on the enlargement shown at right; black dots indicate "nonvisual" cells, white dots "visual" cells; the cells recorded from the anterior bank of parietooccipital sulcus are numbered from 1 to 16. **Bottom:** Receptive fields mapped at different recording sites in areas V1, V2, and V6Ad/V6Av. Ipsi, ipsilateral visual field; contra, contralateral visual field; nv, nonvisual cell; RP, real-position cell; Ls, lunate sulcus; IPs, intraparietal sulcus; POm, medial parietooccipital sulcus; areas V1, V2, V6Av, and V6Ad are also indicated. Other details and abbreviations as for Figure 1.

recognizing which labeled cells in other cortical areas could be due to this unwanted release (for details see Galletti et al., 2001). Cells labeled by leakage of tracer were excluded from the total number of labeled cells obtained from injection sites.

After appropriate survival periods (14 days for FB, DY, CTB red, and CTB green; 10 days for CTB gold; 2 days for WGA-HRP), each animal was anesthetized with ketamine hydrochloride (15 mg/kg i.m.), followed by a lethal i.v. injection of sodium thiopental. They were perfused through the left cardiac ventricle with the following solutions: 0.9% sodium chloride, 3.5–4% paraformaldehyde in 0.1 M phosphate buffer, pH 7.4, and 5% glycerol in the same buffer. The brains were then removed from the skull, photographed, and placed in 10% buffered glycerol for 3 days and in 20% glycerol for 4 days. Finally, they were cut on a freezing microtome at 60 μm in the parasagittal plane, except for two hemispheres (cases 11L and 19L) that were cut in the coronal plane. In cases 18L and 11L, one section of five was processed for HRP histochemistry with tetramethylbenzidine as chromogen (Mesulam, 1982). In cases 17R and 18L, one section of five was processed to reveal CTB gold by the silver-intensification protocol described by Kritzer and Goldman-Rakic (1995). In the remaining cases, one section of five was mounted, air dried, and quickly coverslipped for fluorescence microscopy. In all cases, sections adjacent to HRP- or CTB gold-processed material or fluorescent material were stained with the Nissl method (thionin, 0.1% in 0.1 M acetate buffer, pH 3.7) for cytoarchitectonic analysis, and, in cases 18, A1, and A3, a further series was stained for myelin (Gallyas, 1979).

Data analysis

The criteria used for the definition of injection sites and the identification of retrograde and anterograde labeling have been fully described in previous papers (Galletti et al., 2001; Luppino et al., 2001). The distribution of retrograde and anterograde (for WGA-HRP injections) labeling was plotted in sections every 600 μm, together with the outer and inner cortical borders, by using a computer-based charting system. In this system, two digital transducers were mounted on the X and Y axes of the microscope stage, and the signals were digitized and stored in software developed in our laboratory, written in the LabView language.

We used CARET (Computerized Anatomical Reconstruction and Editing Toolkit; Van Essen et al., 2001; http://brainmap.wustl.edu/caret/) to obtain two-dimensional (2D) and three-dimensional (3D) reconstructions of the cortical surface of the brains used in this study. The process has been described in detail by Galletti et al. (2005). Briefly, we calculated the midthickness contours of each section. All the contours, with the locations of labeled cells, of injection site borders and of cytoarchitectonic borders, were imported into CARET and then manually aligned. CARET generates a 3D reconstruction of the brain and a 2D map by flattening the 3D reconstruction (Van Essen, 2002). Figure 3A–D shows an overview of the location of injection sites and of architectonic borders superimposed on the reconstruction of a representative hemisphere.

Assignment of injection sites. Area V6Ad is bordered ventrally by area V6Av, dorsally by area PEc, medially by area PGm, and laterally by area MIP (see Fig. 1). The injection sites on which the present study is based were attributed to the architectonic areas V6Ad, V6Av, or PEc after careful analysis of adjacent Nissl-stained sections using the cytoarchitectonic criteria fully described by Luppino et al. (2005).

Figure 4 shows the typical cytoarchitecture of area V6Ad together with that of the nearby areas V6Av and PEc. All three areas show a typical parietal pattern, with well-developed layer III, a relatively dense layer IV in which the upper part appears to be somewhat less dense than the lower part, and a layer VI with a blurred border against the white matter. As described in detail by Luppino et al. (2005), in spite of many evident similarities, several cytoarchitectural features differentiate the pattern of V6Ad from that of the nearby areas V6Av and PEc. Area V6Ad shows homogeneous layers III and V, populated by large numbers of medium-sized pyramids, in which only isolated groups of outstanding pyramids are present (see enlargement in the right part of Fig. 4). Area V6Av, in contrast, is characterized by a dense layer III with relatively larger pyramids in its lower part and a layer V populated by relatively large pyramidal cells. Area PEc, in agreement with observations of Pandya and Seltzer (1982), is characterized by the presence of a very clear size gradient in layer III, which is densely populated by medium-sized pyramids in its lower part, and by a dense layer V with a high number of relatively large pyramids.

On the mesial surface of the hemisphere, area V6Ad borders a region that presents a thick and homogeneous layer III, a layer V populated by many small pyramids, and a relatively dark layer VI. This region was described by Pandya and Seltzer as area PGm (Pandya and Seltzer, 1982). Laterally, on the medial bank of IPs, area V6Ad borders a cortical region characterized by a clear increase in the size and density of medium-sized pyramids in layers III and V. This region presumably corresponds to area MIP, as described by different authors on the basis of functional and hodological data (Colby et al., 1988; Colby and Duhamel, 1991), myeloarchitectural analysis (Colby et al., 1988; Rosa et al., 1993; Lewis and Van Essen, 2000), and cytoarchitectural criteria (Luppino et al., 2005).

Assignment of labeled cells. We used different criteria to assign labeled cells to different cortical areas: whenever possible, we recognized the areas on the basis of architectonic patterns previously reported in the literature. When this was not possible, because the plane of sectioning was not perpendicular to the cortex or the lack of a pattern description in the literature, the assignment was essentially based on their brain location, according to previous reports.

In the depth of the parietooccipital sulcus, the labeling was assigned to areas V6 or V6Av according to the cytoarchitectonic criteria defined by Luppino and collaborators (2005) and to areas V2 and V3 when they occupied the posterior bank of the sulcus and were not recognized within the limits of area V6 (see detailed discussion in Galletti et al., 1999a).

In the posterior parietal cortex, the superior parietal lobule was subdivided into areas PEc, PE, and PGm according to the cytoarchitectonic criteria described by Pandya and Seltzer (1982) and recently confirmed by Luppino and coworkers (2005). The cortical convexity of the inferior parietal lobule was subdivided into areas Opt, PG, PFG, and PF according to the cytoarchitectonic criteria described by Pandya and Seltzer (1982) and recently confirmed and extented by Gregoriou and coworkers (2006).

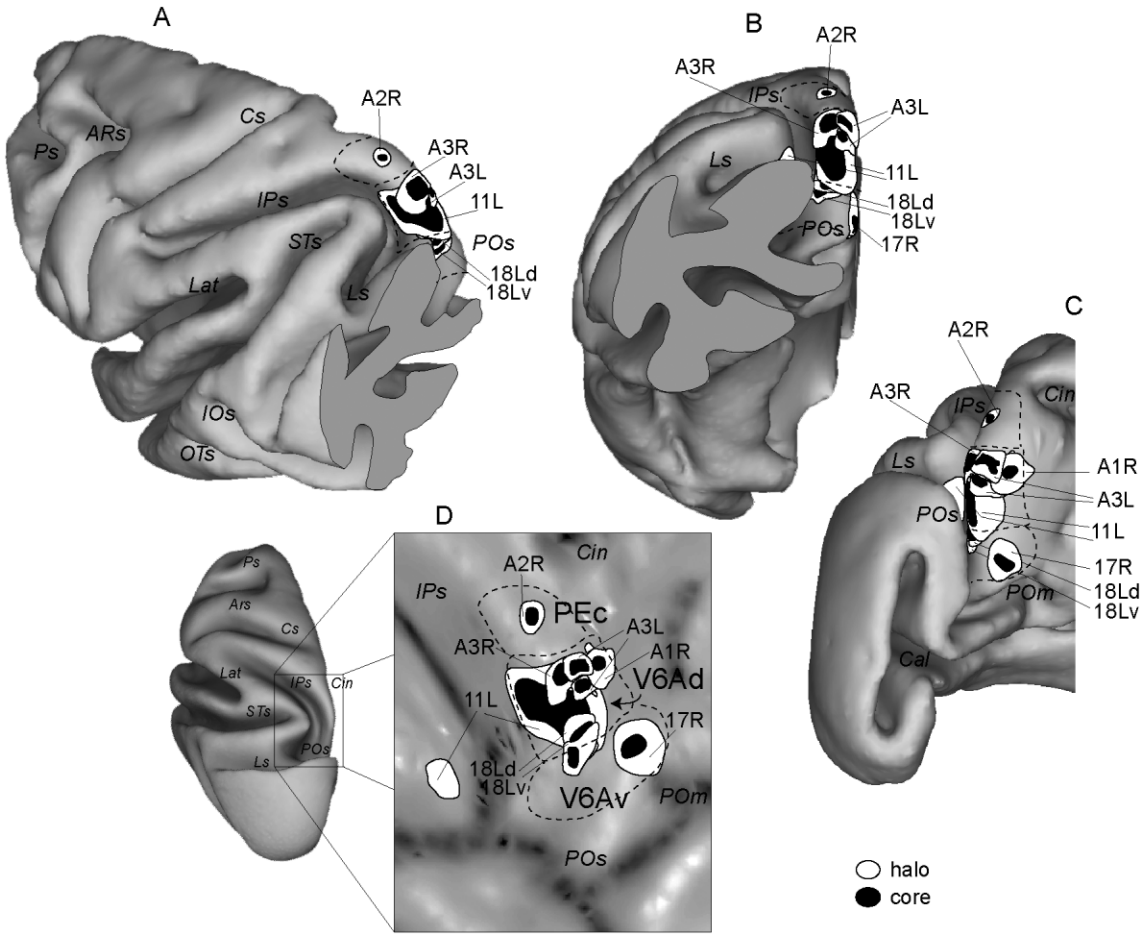

Figure 3.
Summary of injection site locations. Posterolateral (**A**), posterior (**B**), and posteromesial (**C**) views of the surface-based 3D reconstructions of the ATLAS brain with the locations of the injection sites. In A and B, the posterior part of the occipital lobe was cut off in order to visualize the entire extent of the anterior bank of POs. Dashed contours represent the mediated cytoarchitectonic borders of areas V6Av, V6Ad, and PEc of the cases included in this work. **D:** Injection sites shown on a bidimensional reconstruction of the parietooccipital region of the left hemisphere of the ATLAS brain, which is shown slightly enlarged at left. Other details and abbreviations as for Figures 1 and 2.

Within the intraparietal sulcus, labeling found in the lateral bank was assigned to areas LIPd or LIPv according to Blatt and coworkers (1990) and to area AIP according to Murata and others (Murata et al., 2000; Borra et al., 2008). Labeling located in the caudal half of the medial bank of the intraparietal sulcus was attributed to area MIP (Colby et al., 1988), and cells located in the rostral half were assigned to area PEip according to Matelli and collaborators (1998). Finally, cells located in the fundus were considered to be located in area VIP, according to Colby and coworkers (1988).

Labeling located in the superior temporal sulcus was assigned to areas V4T, V5/MT, MST, and FST on the basis of location within the sulcus and myeloarchitectonic patterns (Gattass and Gross, 1981; Gattass et al., 1988; Komatsu and Wurtz, 1988; Boussaoud et al., 1990).

Labeled cells in the depth of the caudalmost segment of the cingulate sulcus were assigned to area PEci according to Pandya and Seltzer (1982). More anterior along this sulcus, labeled cells were assigned to areas 31, 23, or 24 on the basis of their anatomical location and of the cytoarchitectonic pattern of the labeled region (Kobayashi and Amaral, 2000, 2003; Morecraft et al., 2004). When labeled cells were macroscopically located posterior to the genus of the cingulate sulcus, they were assigned to area 31. Anterior to this point, labeling was assigned to area 23 when corresponding to the caudal half of the corpus callosum and to area 24 when corresponding to the rostral half.

Areas of the agranular frontal and prefrontal cortex were classified according to the cytoarchitectonic criteria of Matelli and collaborators (1991) and of Preuss and Goldman-Rakic (1991), respectively.

For more objective information on the relative strength of connections observed in the present study, we calculated the total number of labeled cells in each case, tallying the cells found in each section (every 600 μm) for each brain region where labeled cells were found (Tables 2, 3). We excluded from the total the labeled cells located in the halo zone and within the cytoarchitectonic limits of the injected area (considered as intrinsic connections). Given that the total number of labeled cells in each case was highly variable because of

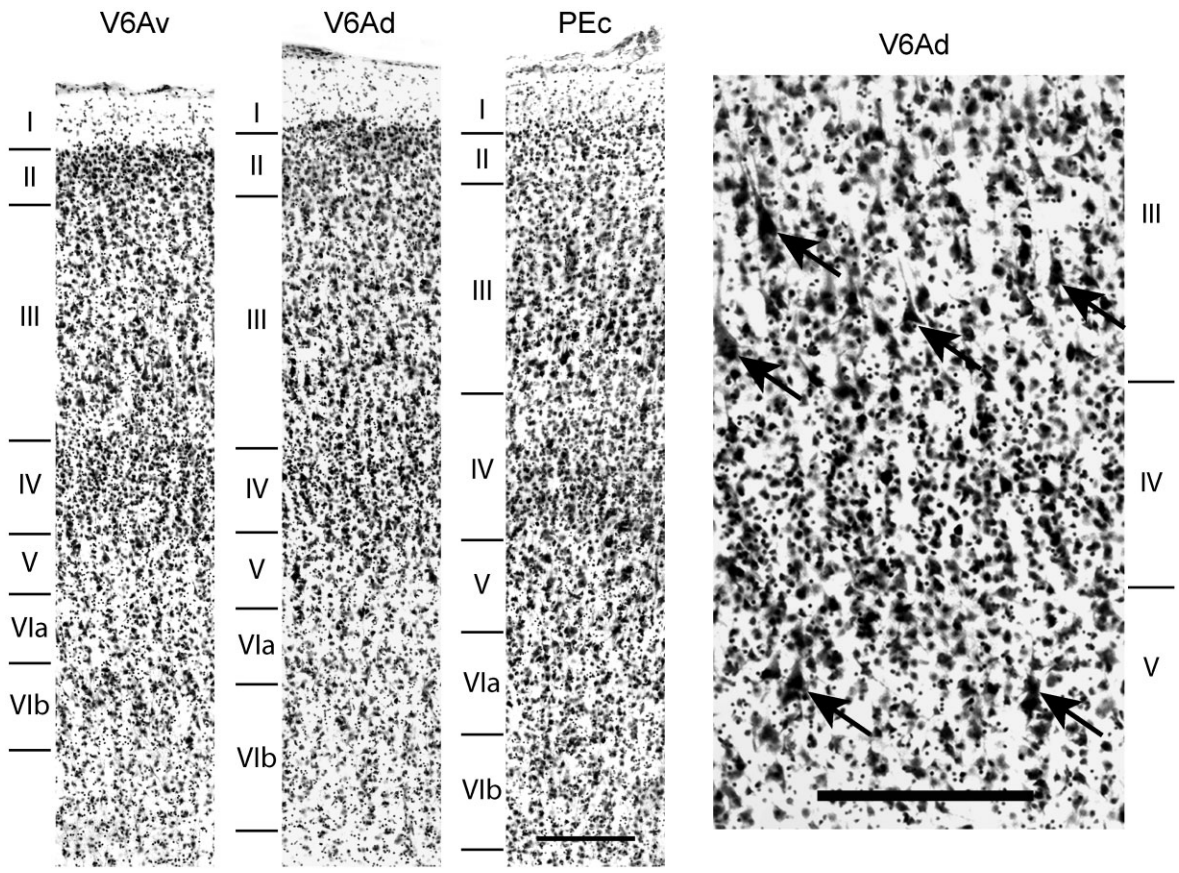

Figure 4.
Cytoarchitectonic pattern of areas V6Av, V6Ad, and PEc. High-magnification views from Nissl section taken at the level of the anterior bank of POs to show the cytoarchitectonic pattern of areas V6Av, V6Ad, and PEc. Image at right is a higher magnification view of V6Ad at the level of III–IV–V layers to show the peculiar aspects of this cytoarchitectonic sector. Arrows indicate some large pyramids standing out from the background of layers III and V. Other details and abbreviations as in Figures 1 and 2. Scale bars = 200 μm.

differences between cases in tracer amount, spread, and transport, the anatomical strength of each connection was expressed in terms of the percentage of labeled neurons found in a given cortical area, with respect to the overall labeling in the given case.

To apply the Abercrombie's correction formula (Abercrombie, 1946) to avoid an overestimation of the total cell counting (see Guillery, 2002), the average cell-body diameters of labeled cells were estimated in each cortical field from photomicrographs captured with a digital camera connected to a Zeiss Axioscope 2 Plus microscope (Axiovision software, v. 4.4; Carl Zeiss, Oberkochen, Germany). Measurements were always made at focal planes approximately corresponding to the center of the soma and were performed by the same observer. We measured at least 20 cells per area in each given section.

The photomicrographs shown in Figure 4 were obtained by capturing images directly from Nissl sections with the same digital camera. Captured images were then imported into Adobe Photoshop, in which they were processed, assembled into digital montages, reduced in the enlargement, and where required adjusted in lighting, contrast, brightness, or sharpness. Data were never altered by this electronic processing.

RESULTS

Eleven tracer injections were placed in eight hemispheres of seven animals (Table 1). Figure 3 shows all the injection sites reported on two- and three-dimensional reconstructions of a common atlas brain. Architectonic analysis of Nissl-stained sections through the injection sites showed that five injections were completely confined within architectonic area V6Ad (see Table 1). Four injection sites involved mainly V6Ad but also, to a variable extent, one or the other of the two nearby areas, V6Av and PEc (see Table 1). Furthermore, in one case (case A2R), the injection site was entirely confined to area PEc, and, in another case (case 17R), the great majority of tracer was released into area V6Av, with small contamination of areas V1 and V2 in the occipital pole.

The connectivity pattern of area V6Ad will be described here on the basis of the results observed in those cases in which the injections sites were entirely circumscribed within the limits of area V6Ad (Table 2). These data will be then compared with the connectivity patterns emerging from tracer injections in either PEc or V6Av (see Table 2). Finally, data from injections that crossed the borders between V6Ad and V6Av or between V6Ad and PEc (four cases; see Table 3) will be briefly decribed.

TABLE 2. Summary of Connections for Injections Within the Cytoarchitectonic Limits of V6Ad, V6Av, and PEc[1]

Injected Area	V6Ad				V6Av	PEc
Case	11L	A3R	A3L[2]	A1R	17R	A2R
POcc						
V3A					++ +	
V4/DP					+++	
V6					++++	
STs						
V4T					++	
V5/MT					++	
MST	++	+++		++	++	
FST					++	
SPL						
V6Av	++	++++	++	++	*	
V6Ad	*	*	*	*	+++	+++
PEc	+++	++++	+++	++		*
PE						+++
Mes ctx						
PGm	+++	++	+++	+++	+++	++
31	++	++	++	++	++	
PEci	+			+	++	++
23	+	++	++		++	+++
24	+	+	+	++		++
IPs						
MIP	+++++	+++++	+++++	+++	++++	+++++
PEip	++	+		+		
VIP	+++	++	+		++	
LIP	++	+	+	++++	++	
AIP	++	++	+++	+		
IPL						
Opt	+	++		++		
PG	++	+++	+++	+++		++
PFG	+	+		+		+++
Front ctx						
F2	+++	++	+++	++		+++
F3	+					++
F5	++		+			
F6	+	+	+	+		
F7		+	++	+++		++
FEF		+		++		
46	+	++		+++		
Total n	103,005	5,378	5,423	9,149	11,977	1,977

[1]Location of injection sites, strength of the labeling, and total number of labeled cells are indicated. The total number of labeled cells was corrected using the Abercrombie formula (Abercrombie, 1946; Guillery, 2002). We scored five levels of connections as high (+++++: >30% of labeling), dense (++++: >15% to <30% of labeling), moderate (+++: >5% to <15% of labeling), light (++: ≥1% to <5% of labeling), and sparse (+: <1% of labeling). *, Areas involved by the injection site.
[2]A3L includes two different injections.

TABLE 3. Summary of Connections for Injections Involving V6Ad, but Partly Involving also the Nearby Areas V6Av or PEc[1]

Injected Area	PEc (V6Ad)	V6Ad (PEc)	V6Ad (V6Av)	V6Av (V6Ad)
Case	A3R	19L	18Ld	18Lv
POcc				
V3A			+++	++
V6		++	+++	+++
STs				
V4T			+++	++
V5/MT			+++	++
MST		++	+++	++++
FST			+++	++
SPL				
V6Av			*	*
V6Ad	*	*	*	*
PEc	*	*	++	
PE	+++			
Mes ctx				
PGm	+++	++++	++	++
31	++++			
PEci		++++	+++	
23	+++++	++		
24		++		
IPs				
MIP	+++		+++	++++
PEip		++	++	++
VIP		+++	+++	+++
LIP				++
IPL				
Opt		++		
PG	+++	+++	+++	+++
Front ctx				
F2		+++	+++	
F4		++		
F7		++		
46	++	++		
Total n	233	12352	1805	963

[1]In case 18L, with two injections, the letter "d" indicates the dorsalmost injection (mainly in area V6Ad) and "v" the ventralmost one (mainly in area V6Av). Labeling <1% were not reported. Other details as in Table 2.

Injections in area V6Ad

Figures 5–8 illustrate the cortical connections observed in three cases with injection sites entirely located in area V6Ad. In case 11L (Figs. 5, 6), two nearby injections of WGA-HRP were placed in V6Ad (see Table 1) using vertical trajectories passing through the exposed cortex of the SPL. The resulting combined injection site involved a large part of V6Ad, sparing only its ventromedial part (see Figs. 3D, 5A–D, 6). The cytoarchitectonic analysis showed that the core of injection site was completely within the limits of area V6Ad (Figs. 5B, 6) and did not involve the underlying white matter (see Fig. 5B,C). The halo zone involved a large part of V6Ad and marginally invaded V6Av, MIP, and superficial layers of a very small region of the lateral bank of IPs (Fig. 5A–D).

As expected from the size of the injection site and the amount of tracer we injected, the number of labeled cells observed in this case was very high. Densely packed labeled cells were found on the medial bank of the intraparietal sulcus (area MIP) and on the mesial surface of the hemisphere (area PGm; Figs. 5E–G, 6). Labeling covered very large extents of both areas and represented, as a whole, more than half of the total number of labeled cells in this case (Table 2).

Because the border between V6Ad and MIP along the medial bank of IPs is not easily recognizable in a coronal plane, this plane being almost tangential to the areal border, we cannot exclude that the tracer's MIP contamination was a bit larger than we recognized. However, because in case A3L the tracer certainly did not involve area MIP (see Figs. 3, 8) and the case presents about the same percentage of labeled cells in area MIP as case 11L (see Table 2), we believe that MIP contamination in case 11L, if any, was only marginal.

About 6% of labeled cells were also found in the nearby area PEc (Figs. 5C–E, 6), which contained label throughout its rostrocaudal extent, though restricted to the medial part of the area. The number of labeled cells assigned to area PEc is likely to represent an underestimate, given that PEc borders the injected area and therefore was partially included in the

Figure 5.
Location of injection site in case 11L (V6Ad injection) and cortical distribution of retrogradely labeled cells. The 3D reconstruction at top left shows the location of injection site in a posterolateral view of the ATLAS brain by CARET. Coronal sections of the brain were taken at the levels indicated on the brain silhouette shown at bottom left. The center of the injection site is at the level of section B. Each black dot represents a labeled cell after WGA-HRP injection in area V6Ad. Hatched areas around the injection site in sections A–D indicate the regions not taken into account in quantitative analysis because they are considered as "intrinsic" connections. Dashed lines on sections represent the cytoarchitectonic borders of areas V6, V6Av, and V6Ad. Areas PEci, MST, LIPv, Opt, PG, 31, 23, 24, AIP, F2, F3, F5, F6, F7, and 46 are indicated. Other details and abbreviations as for Figures 1–3.

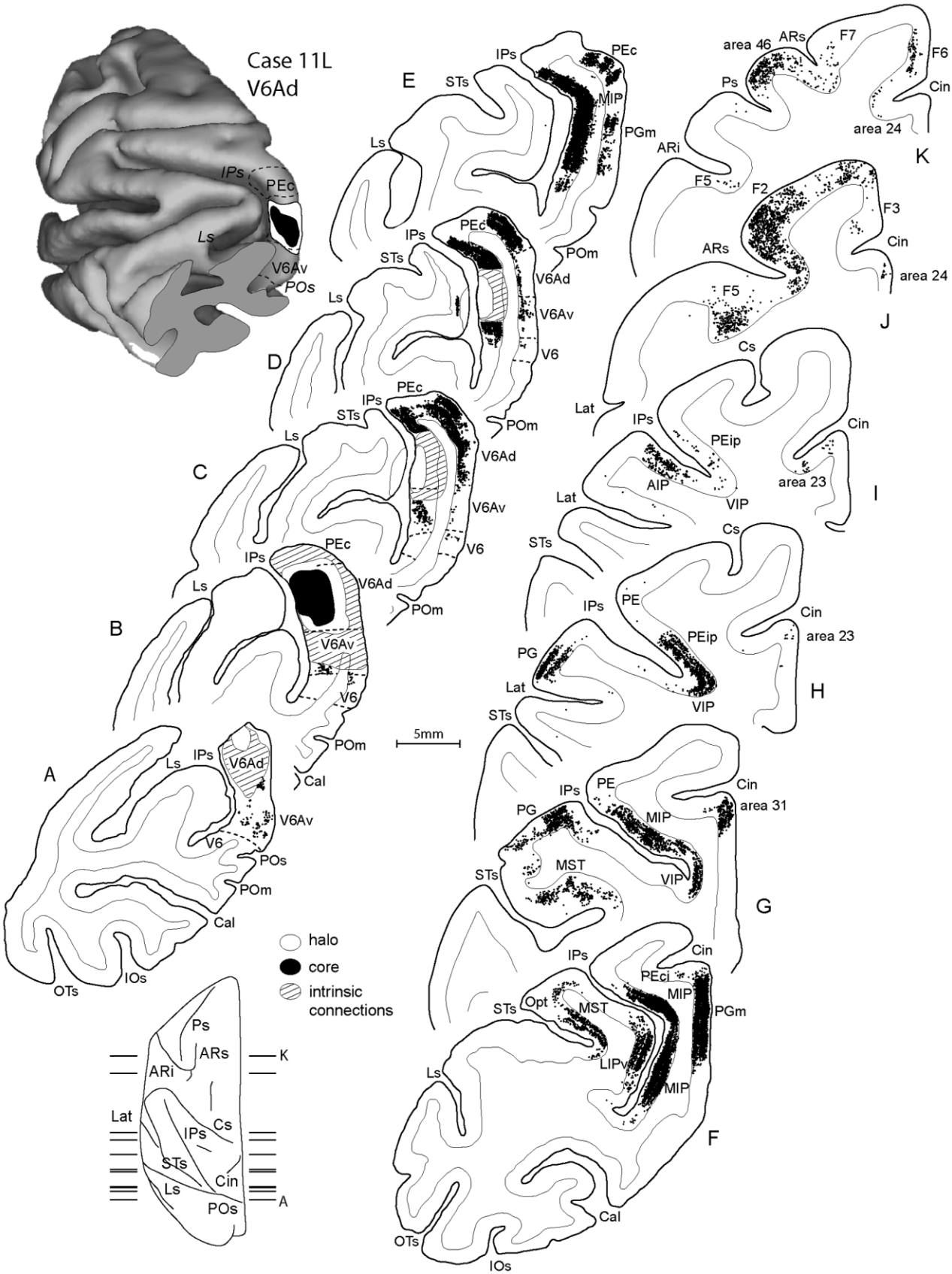
Case 11L
V6Ad
IPs
PEc
Ls
V6Av
POs
A
B
C
D
E
F
G
H
I
J
K
STs
MIP
PGm
POm
V6Ad
V6Av
V6
PE
PEip
VIP
AIP
PG
MST
LIPv
Opt
PEci
Cin
area 31
area 23
area 24
area 46
F7
F6
F5
F2
F3
ARs
ARi
Ps
Cs
Lat
Cal
OTs
IOs
5mm
halo
core
intrinsic connections

Figure 5

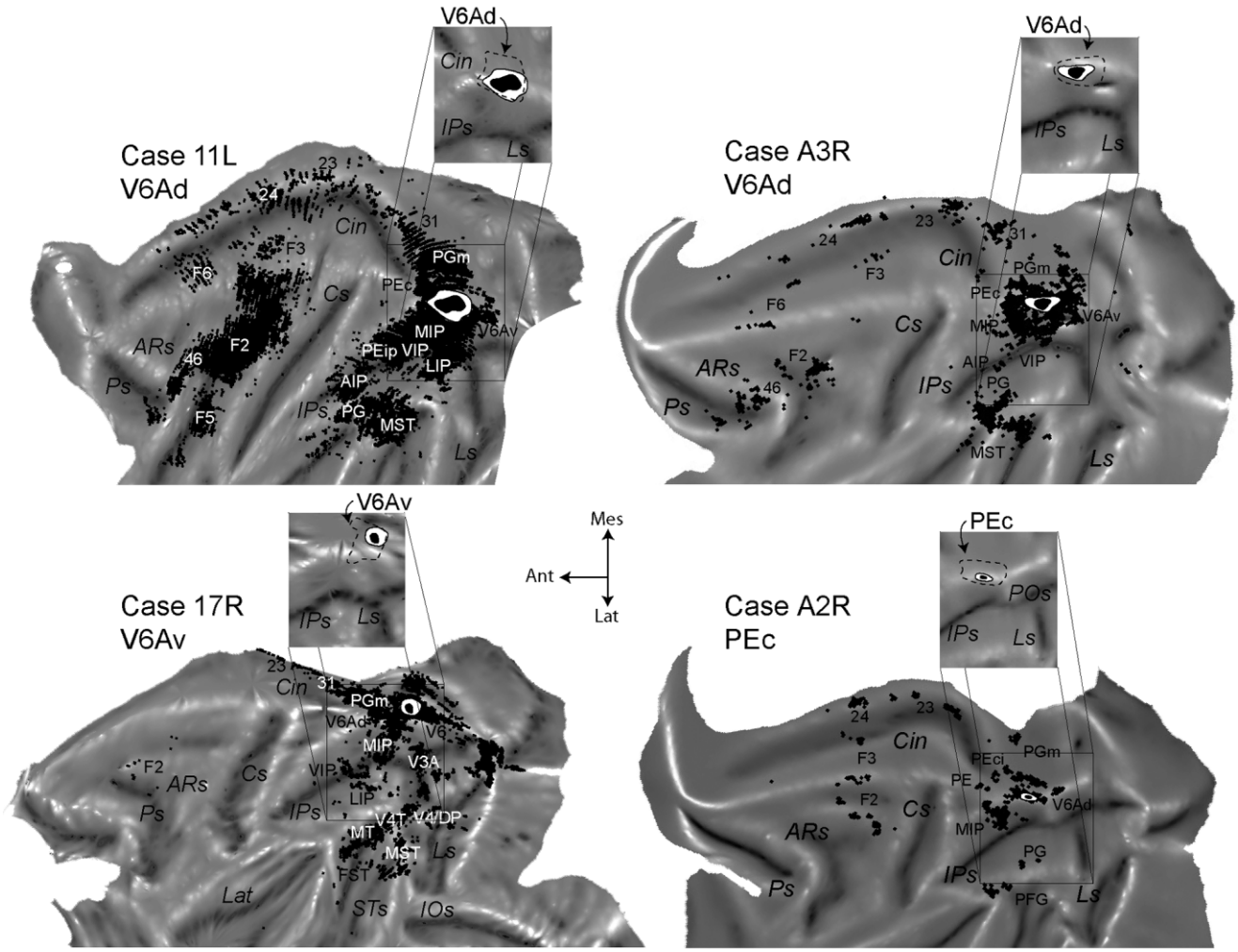

Figure 6.
Bidimensional reconstructions of four cases with injections in V6Ad (two cases), V6Av, and PEc. **Top:** Bidimensional maps of cases 11L and A3R with injection in V6Ad. Only maps of the dorsal part of the brain are given, with the location of labeled cells indicated as black dots. Dashed contours around the injection sites indicate the cytoarchitectonic borders of area V6Ad. **Bottom:** Bidimensional maps of cases 17R and A2R with injection in V6Av and PEc, respectively. Details as in the top part. Abbreviations as for Figures 1, 2, and 5.

heavily labeled region we represented as "intrinsic connections" (see Fig. 5B).

Most of the remaining labeled cells were found in areas located in the frontal lobe. Most of this label was in the dorsal premotor cortex, especially in the ventral and rostral part of the caudal area F2 (F2vr; Figs. 5J, 6), extending into the caudal part of area F7 (Fig. 5K). Additional, minor labeling was observed in areas F3 (Figs. 5J, 6), F6 (Figs. 5K, 6), and F5 in the depth of the posterior bank of the inferior arcuate sulcus (Figs. 5J,K, 6). Finally, in the prefrontal cortex, labeling was observed in the dorsal part of area 46 (Fig. 5K).

Several labeled cells were found in areas MST (Figs. 5F,G, 6), LIP (Figs. 5F, 6), VIP (Figs. 5G–I, 6), PEip (Figs. 5H,I, 6), AIP (Figs. 5I, 6), Opt and PG on the exposed surface of IPL (Figs. 5F–H, 6), and in area 31 (Figs. 5G, 6). Patches of labeled cells were also found in areas 23 and 24 along the cingulate sulcus (Figs. 5H–K, 6) and in area V6Av (Figs. 5A–D, 6). Rare labeled cells were found in area V6 at the border with V6Av (Fig. 5B–D).

Figures 7 and 8 show two cases (A3R, A3L) in which the injection sites involved the central, dorsal part of area V6Ad. Because the two hemispheres were cut in the sagittal plane, the analysis of cytoarchitecture was difficult in sections close to the mesial surface of the hemisphere and in proximity to the medial bank of the intraparietal sulcus. Altogether, the distribution of labeling observed in these two cases was congruent with that observed in case 11L.

Figures 6 and 7 (case A3R) show an FB injection in the most dorsal and central part of area V6Ad. It was entirely within the cytoarchitectonic limits of this area. The tracer was released mainly in the supragranular layers, and only the halo zone of injection involved infragranular layers. The strongest connection was with area MIP (Figs. 6, 7E,F). Many labeled cells were also found in areas PEc (Figs. 6, 7A–F) and V6Av (Figs. 6, 7A–F). Consistent patches of labeled cells were found in MST (Figs. 6, 7G), PGm (Figs. 6, 7A–C), and PG (Figs. 6, 7H), as well as in some areas located within the IPs, such as VIP, LIP, and AIP (Figs. 6, 7F–H). Patches of labeled cells were found in

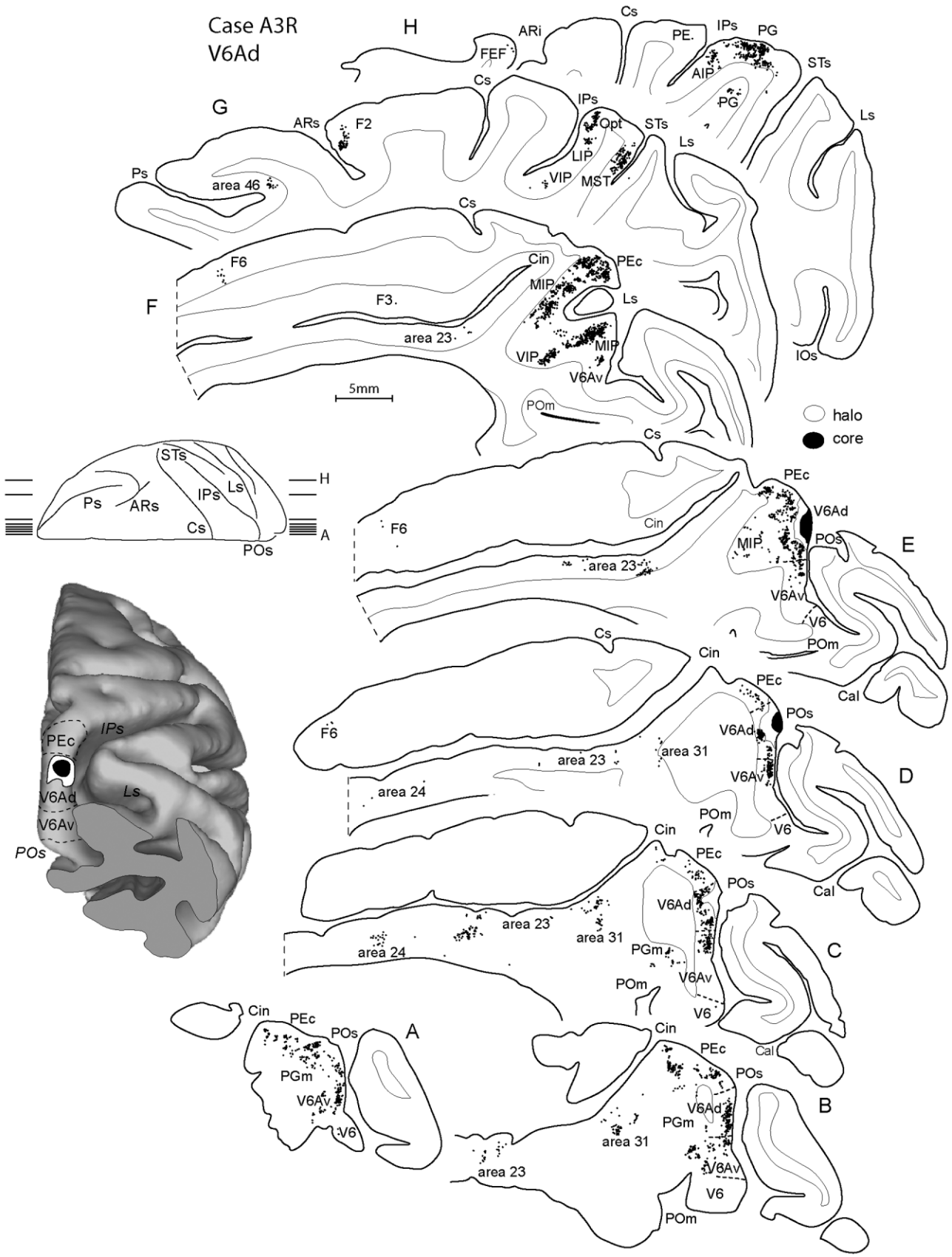

Figure 7.
Location of injection site in case A3R (V6Ad injection) and cortical distribution of retrogradely labeled cells. Sagittal sections of the brain were taken at the levels indicated on the brain silhouette shown in the center. Each black dot represents a labeled cell after FB injection in area V6Ad. FEF, area FEF. Other details and abbreviations as for Figures 1–3 and 5.

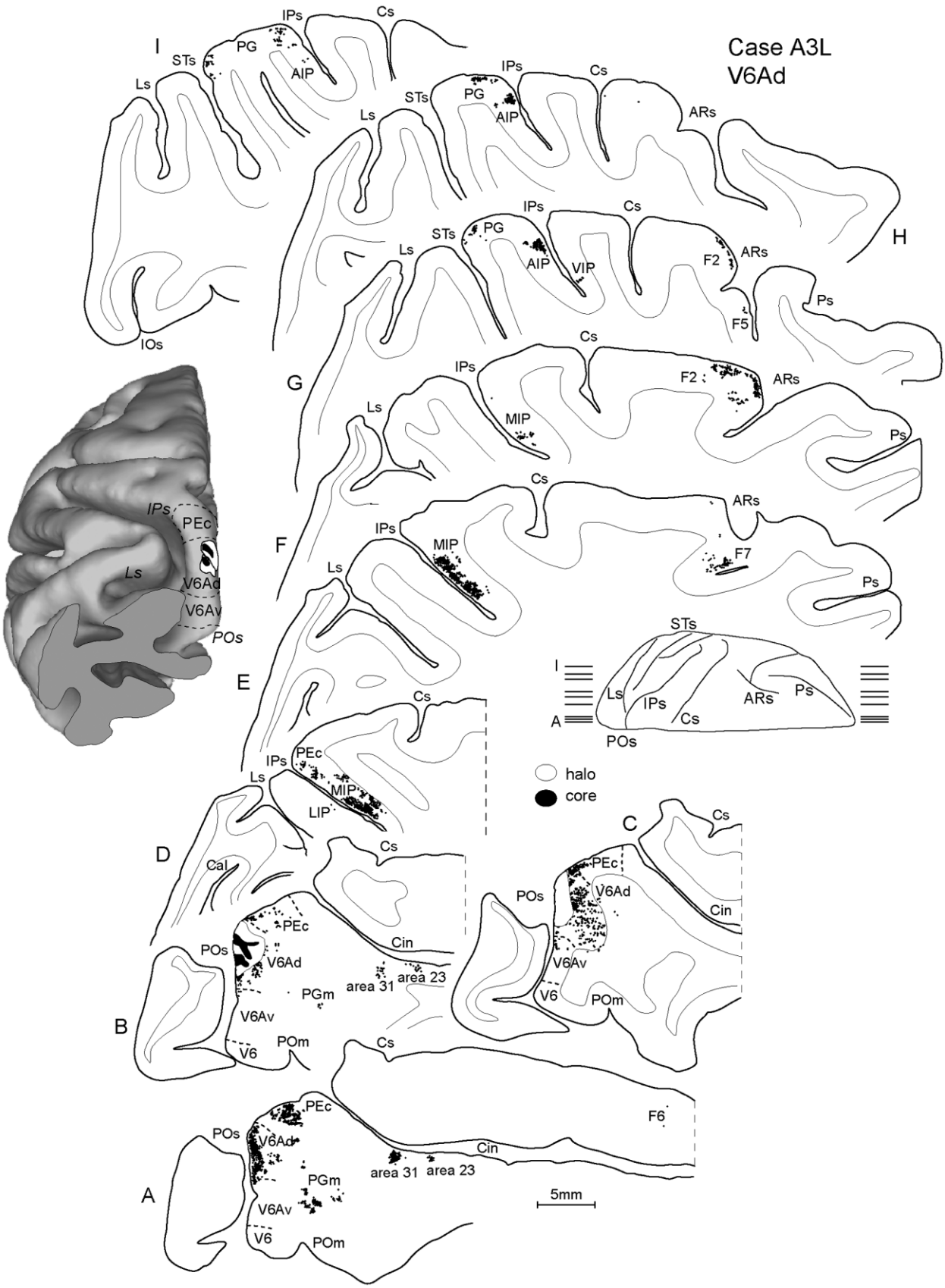

Figure 8.
Location of injection sites in case A3L (V6Ad injection) and cortical distribution of retrogradely labeled cells. Sagittal sections of the brain were taken at the levels indicated on the brain silhouette shown in the center. Black dot represents labeled cells after injections of either CTB red (dorsalmost injection) or CTB green (ventralmost injection), both within the limits of area V6Ad. Other details and abbreviations as for Figures 1–3 and 5.

areas F2vr and 46 in the frontal lobe (see Figs. 6, 7G), whereas more scattered labeled cells were observed in area F6 (Figs. 6, 7D–F). Patches of labeled cells were also found in the cingulate areas 23 and 24 (Figs. 6, 7B–F) and in area 31 (Figs. 6, 7B–D).

In case A3L (Fig. 8), two small injections (see Table 1) were carried out close to each other in the mediodorsal part of anterior bank of the parietooccipital sulcus. In the more dorsal one CTB red was injected, and in the ventral one CTB green. Because both injections were within the cytoarchitectonic limits of V6Ad, we illustrate in Figure 8 all labeled cells regardless of which tracers they contained.

The strongest connection was again with area MIP (Fig. 8D–F). Many labeled cells were also seen in area PEc (Fig. 8A–D), whereas much less intense labeling was detected in V6Av (Fig. 8A–C). In the intraparietal sulcus, relatively dense patches of labeled cells were found in AIP (Fig. 8G–I), whereas VIP contained a few labeled cells (Fig. 8G). On the mesial surface of the hemisphere, consistent patches of labeled cells were found in areas PGm (Fig. 8A,B) and 31 and in area 23 on the ventral bank of the cingulate sulcus (Fig. 8A,B). Less intense but consistent was the labeling in area PG (Fig. 8G–I) on the exposed cortex of inferior parietal lobule. In the frontal lobe, many labeled cells were found in area F2 (Fig. 8F,G), with less dense labeling in area F7 (Fig. 8E). A few labeled cells were located in area F5 (Fig. 8G).

In the last case of V6Ad injection (case A1R, CTB red; not illustrated except for the location of the injection site in Fig. 3), the injection site was located at the level of the exposed V6Ad on the mesial surface of the hemisphere. Also in this case the strongest connections were with areas MIP and PGm, but unlike other cases the connection with area LIP was very strong. Many labeled cells were seen in areas PEc, MST, and V6Av. Connections were observed in the inferior parietal lobule with area PG and less intensely with area Opt and in the frontal lobe with areas F2, F7, FEF, and 46. Less intense but consistent were the connections with areas 31 and the cingulate area 24.

Quantitative analysis

Figure 9 summarizes the quantitative analysis carried out on the four cases in which tracer was entirely released within the cytoarchitectonic limits of area V6Ad. Labeled areas have been grouped according to their brain location. Only cortical areas containing more than 1% of the total labeled cells are displayed. The variability across individual cases (see Table 2), reported as standard deviation in Figure 9, can be accounted for by the use of different tracers, by a differential laminar involvement of injection sites, and/or by the marginal spread of halo zone of injection sites into neighboring areas.

Data reported in Figure 9 represent about 95% of the total labeled cells, so they should be considered as representative of the cortical connectivity pattern of area V6Ad. Note that afferents from area MIP form by far the most numerous V6Ad connections, representing about 35% of the total. Strong afferences (each of them representing 5–10% of the total) are also those from areas PEc, PGm, LIP, PG, and F2. It is interesting to note that neither the primary visual area nor the classic extrastriate areas are directly connected with V6Ad. Visual inputs to V6Ad come from areas MST, VIP, and V6Av.

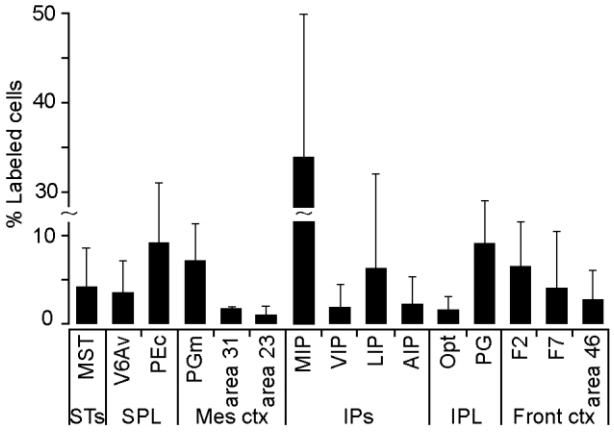

Figure 9.
Main cortical connections of area V6Ad. Average percentage (with SD) of labeled cells in different cortical areas after tracer injection in area V6Ad. Only cases with injection within the cytoarchitectonic limits of area V6Ad were taken into account. Percentages <1% are not reported. Connected cortical areas are grouped on the basis of their brain location. SPL, superior parietal lobule; Mes ctx, mesial cortex; IPL, inferior parietal lobule; Front ctx, frontal cortex. Other details and abbreviations as for Figures 1, 2, 5, and 7.

Injections in areas adjoining V6Ad

Injection in area V6Av. In one case (case 17R; Figs. 6, 10), neuronal tracer was injected in the ventral part of area V6A (cytoarchitectonic field V6Av; Luppino et al., 2005). The tracer (CTB gold) was injected with a recording syringe (see Materials and Methods). The bottom right part of Figure 10 shows the type of cells and the receptive fields encountered along the penetration. There was a small leakage of tracer in areas V1 and V2 (Fig. 10A). The receptive fields mapped in the region of tracer leakage were located at about 6 (area V1) and 9 (area V2) degrees of eccentricity (see bottom right part of Fig. 10). To be conservative, we therefore excluded from the count of labeled cells those cells in striate and extrastriate visual areas that were located in the region of 5° to 10° representation (according to the well-known topography of visual areas; see Daniel and Whitteridge, 1961; Gattass et al., 1981, 1988).

The location of the injection site (the ventralmost part of the anterior bank of parietooccipital sulcus; Figs. 6, 10B) was where area V6 was usually found (Galletti et al., 1999a). However, the functional recognition of the cortex passed through with the recording syringe, and in particular the presence of several cells insensitive to the visual stimulation (Galletti et al., 1996, 1999b), as well as the *post-mortem* cytoarchitectural analysis of the cortical region in and around the injection site clearly indicated that this injection was mainly in area V6Av.

Afferences to V6Av come from the extrastriate visual areas V3A, V4/DP, V4T, V5/MT (Figs. 6, 10E,F); the parietal areas V6Ad (Figs. 6, 10A–C), MST (Figs. 6, 10E,F), MIP, LIP, VIP (Figs. 6, 10C,D); and the mesial areas PGm and 31 (see Figs. 6, 10A,B), 23 (Figs. 6, 10B), and PEci (Figs. 10A–C). Area V6Av is not connected with PEc, and only few cells were found in the inferior parietal lobule and in the frontal lobe.

Injection in area PEc. In one case, a small injection of neuronal tracer (CTB green) was entirely confined within the cytoarchitectonic limits of area PEc (case A2R; Figs. 6, 11).

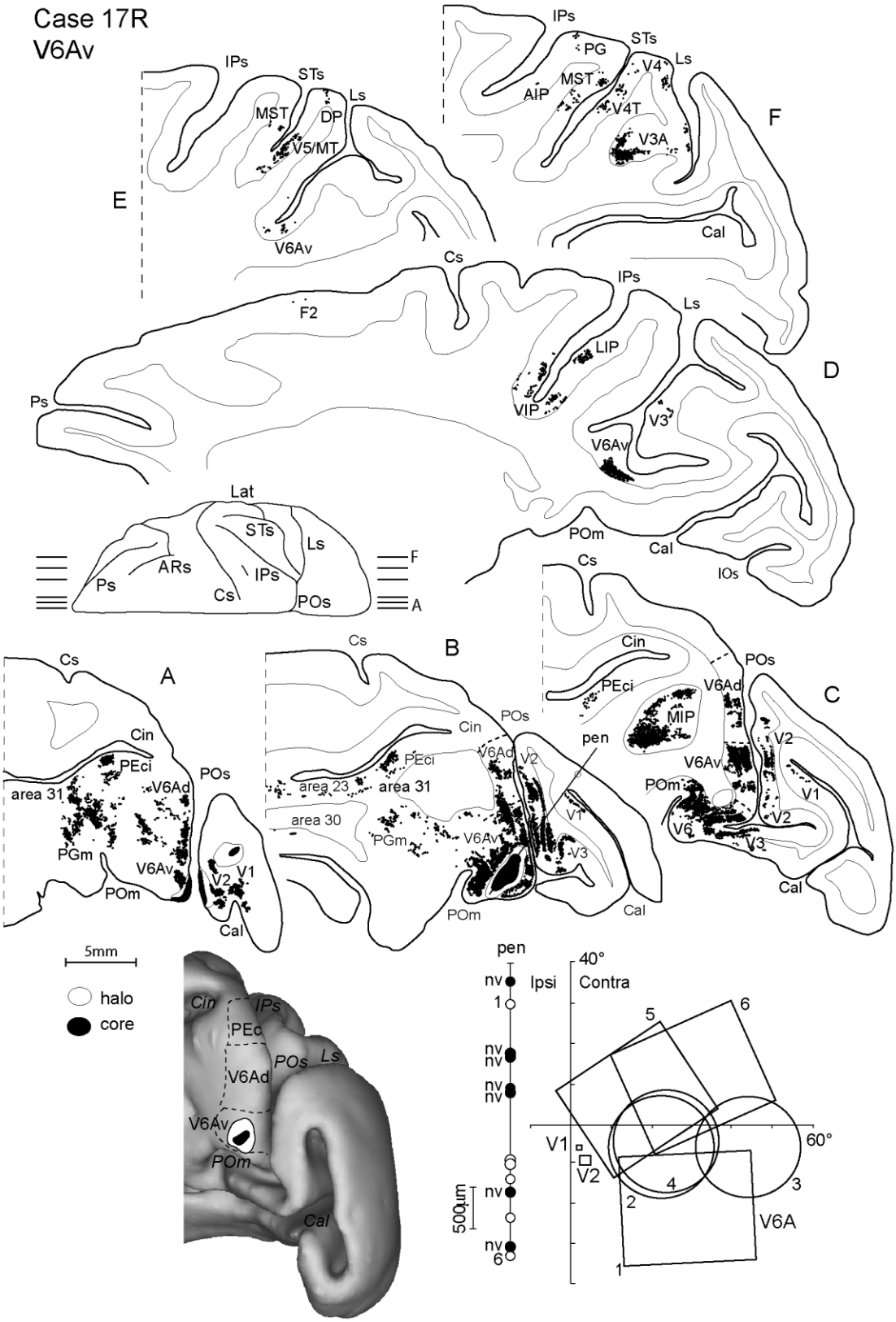

Figure 10.
Location of injection in case 17R (V6Av injection) and cortical distribution of retrogradely labeled cells. Sagittal sections were taken at the levels indicated on the brain silhouette shown at the center. Each black dot represents a labeled cell after CTB gold injection in area V6Av. At bottom right, the receptive fields mapped at different recording sites in areas V1, V2, and V6Av are reported (microelectrode penetration is reconstructed in section B). Other details and abbreviations as for Figures 1–3 and 5.

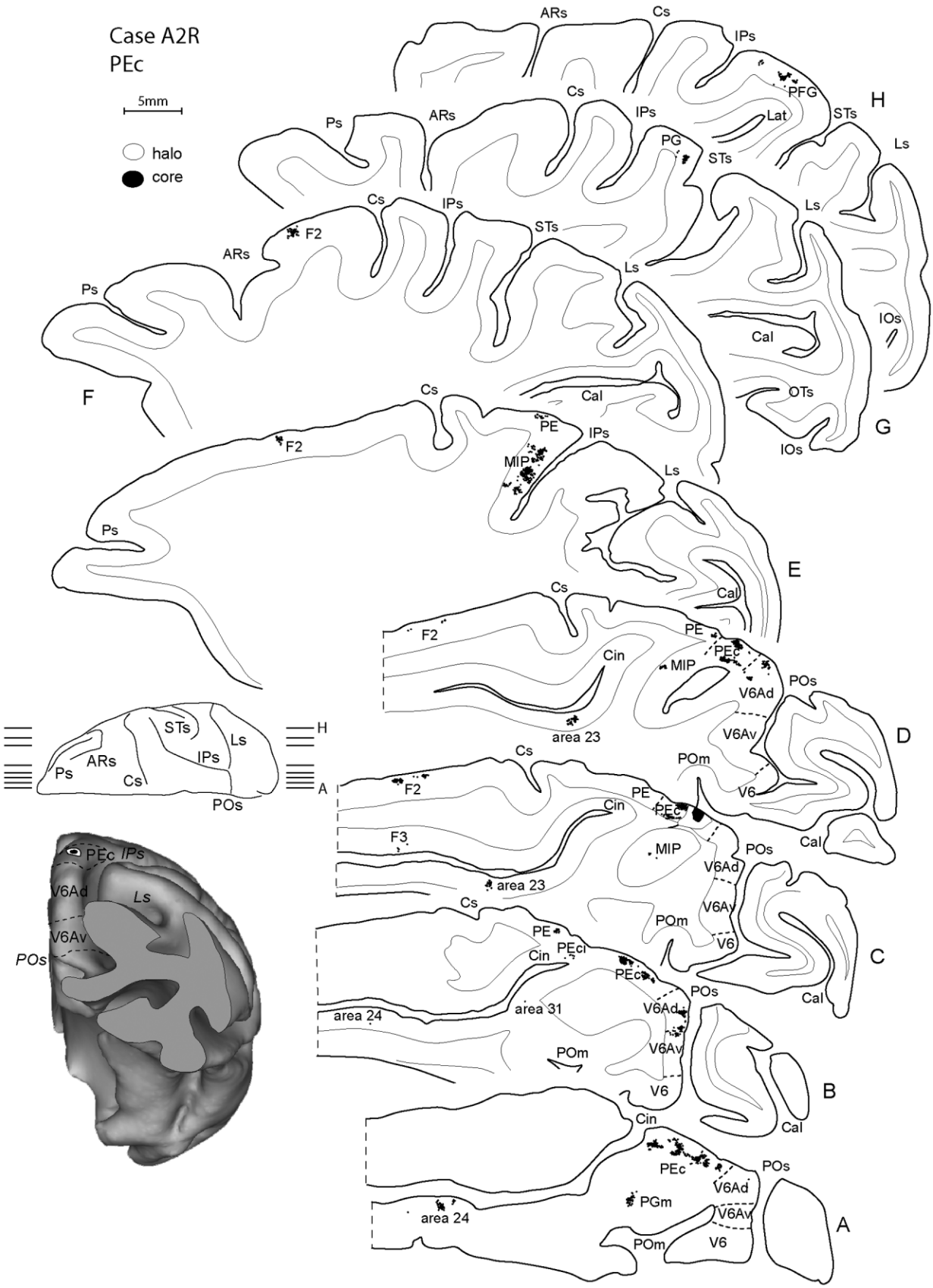

Figure 11.
Location of injection site in case A2R (PEc injection) and cortical distribution of retrogradely labeled cells. Sagittal sections were taken at the levels indicated on the brain silhouette shown at the center. Each black dot represents a labeled cell after CTB green injection in area PEc. Other details and abbreviations as for Figures 1–3 and 5.

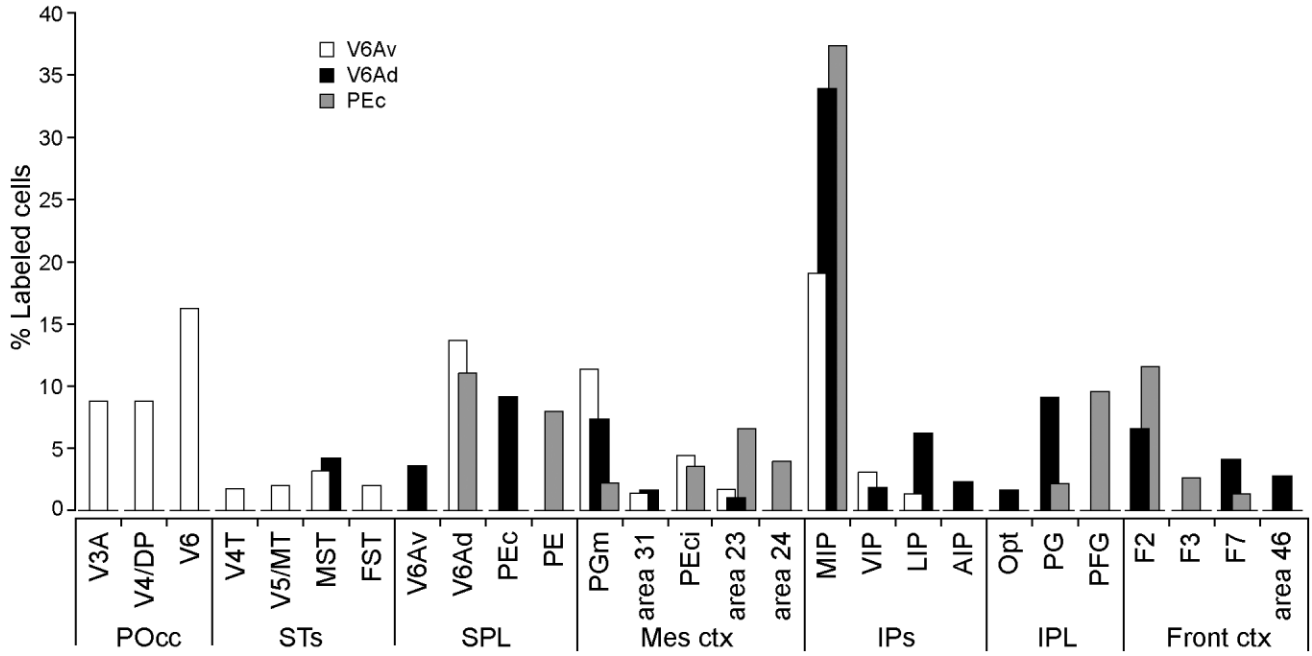

Figure 12.
Comparison of cortical connections of V6Av, V6Ad, and PEc. Average percentage of labeled cells in different cortical areas after tracer injection in V6Av, V6Ad, and PEc. POcc, parietooccipital cortex. Other details and abbreviations as for Figures 1 and 9.

The strongest connection of PEc was with area MIP (Figs. 6, 11E). Consistent connections were also found with areas V6Ad (Figs. 6, 11B–D), PE (Figs. 6, 11B–E), PGm (Figs. 6, 11A), PEci, 31, 23, and 24 along the cingulate sulcus (Figs. 6, 11A–D), areas PG and PFG in the exposed cortex of IPL (Figs. 6, 11G,H), and area F2 in the frontal lobe (Figs. 6, 11C–F). A few labeled cells were also found in area F3 (Figs. 6, 11C). Apart from area MIP, no labeled cells were found in areas located within the intraparietal sulcus.

Figure 12 compares the pattern of cortical connections of area V6Ad with the above-mentioned preliminary data obtained after injections in areas V6Av and PEc, e.g., the two nearby areas that border V6Ad posteriorly and anteriorly, respectively. In Figure 12, areas containing labeled cells are grouped together according to their brain location (as in Fig. 9).

Area V6Ad is strongly connected with several areas of the intraparietal sulcus and of the superior and inferior parietal lobules and with areas of the mesial and frontal cortices. V6Ad receives consistent projections from only one area of the superior temporal sulcus, the MST.

Area V6Av has much stronger connections with visual areas than V6Ad does, receiving about 35% of its visual input from parietooccipital extrastriate areas and another 10% from visual areas of the superior temporal sulcus. No labeling was observed in the dorsal premotor cortex or in area Opt, which did not conform to expectations from previous reports (Luppino et al., 2005; Rozzi et al., 2006). This discrepancy could be accounted for by the medial location of the injection site in area V6Av or by an incomplete cortical laminar involvement by tracer deposit.

The two cases in which tracer injection included both V6Ad and V6Av (18Ld and 18Lv; see Table 3) confirm the difference in pattern of connections between these two areas. Note that neither injection involved the occipital pole, and both were too dorsal to involve area V6. Therefore, the labeled cells observed in the visual areas after V6Av injection but not after V6Ad injection (Table 2) cannot be ascribed to the tracer involvement of other visual areas passed through by the recording/injecting syringe but instead represent an actual difference in connection between the two areas. As shown in Table 3, both injections in case 18L present strong connections with extrastriate visual areas, likely as a result of the involvement in both cases of V6Av (see the very ventral location of both injection sites in Fig. 3). On the other hand, only in case 18Ld (injection mainly in V6Ad) was there labeling in areas PEc and F2, which are typical targets of V6Ad and are not labeled after V6Av injection. Although these data indicate a clear difference between cortical connections of V6Ad and V6Av, we are aware that further experiments are needed to identify all the specific aspects of the connectivity of area V6Av.

Area PEc shares several connections with V6Ad but also displays many consistent differences. In particular, PEc is not connected with areas MST, V6Av, 31, VIP, LIP, AIP, Opt, or 46, which in contrast are connected with V6Ad. PEc is also connected with areas PE, PEci, 24, PFG, and F3, all areas that are not connected with V6Ad. The comparison between cortical connections of V6Ad and PEc, like that between V6Ad and V6Av, represents a preliminary analysis; a comprehensive study of PEc connections will be necessary for verification.

Laminar pattern of connections

Other authors (Rockland and Pandya, 1979; Maunsell and Van Essen, 1983) have suggested that the laminar pattern of labeled cells is a useful tool for determining the hierarchical

TABLE 4. Percentage of Cells in the Supragranular Layers (%Supra) After Injections in V6Ad[1]

V6Ad injections	%Supra 11L	%Supra A3R	%Supra A3L	%Supra A1R	%Supra average	Type of distribution
STs						
MST	39	72		70	60	B
SPL						
V6Av	74	87	94	95	88	S
PEc	49	69	75	55	62	B
Mes ctx						
PGm	48	67	32	26	43	B
31	53	40	87	48	57	B
23	41	51	100	60	63	B
IPs						
MIP	55	66	84	35	60	B
VIP	59	19	79		52	B
LIP	59	100	86	77	81	S
AIP	81	87	91	56	79	S
IPL						
Opt	39	67		47	51	B
PG	45	67	90	57	65	B
Front ctx						
F2	55	63	95	86	75	S
F7	27	0	74	51	38	B
46	57	69		78	60	B

[1]The calculations were based on data obtained from four cases with injections within the cytoarchitectonic limits of V6Ad. Only data of areas with an average labeling >1% are reported. S, supragranular distribution (%Supra >70%); B, bilaminar distribution (%Supra between 30% and 70%; Rockland and Pandya, 1979; Maunsell and Van Essen, 1983).

level of the labeled area with respect to the injected area. According to this view, a high percentage of labeled cells in supragranular layers would indicate feed-forward projections (hence lower hierarchical level) and a high percentage of labeled cells in infragranular layers feed-back projections (hence higher hierarchical level). We checked the laminar patterns of retrograde labeling after V6Ad injections. The results of this study are reported in Table 4. Most of the target areas are located at the same hierarchical level of area V6Ad (pattern B: supragranular labeled cells between 30% and 70%, Maunsell and Van Essen, 1983). Four areas (V6Av, LIP, AIP, F2) are located at a lower level with respect to V6Ad (pattern S: supragranular labeled cells >70%). There were no cortical areas connected with V6Ad, with the percentage of labeled cells in supragranular layers lower than 30%, a value suggesting that the area would be at a higher hierarchical level with respect to V6Ad (Rockland and Pandya, 1979; Maunsell and Van Essen, 1983). These results would indicate that only four cortical areas feed-forward information to V6Ad. Likely, visual information comes from V6Av, oculomotor and attentional information from LIP, and grasping and reaching information from AIP and F2. Even if these afferences seem difficult to reconcile with a strictly caudal-to-rostral hierarchical scheme, other extrastriate areas (Vezoli et al., 2004; Burman et al., 2006), such as V6Ad, show similar behavior.

Injection sites including two cortical areas

In four cases, the cytoarchitectonic analysis carried out to trace the border of V6Ad showed that tracer injections were centered in V6Ad but also invaded a nearby area. As reported in Table 3, the pattern of connection of these mixed cases mirrored that of cases with injections in single areas. Case 19L (mainly V6Ad, but also PEc) shows connections similar to those with injection in V6Ad, together with additional connections that can be attributed to PEc (for instance, PEci afferences). In case A3R (mainly PEc, but also V6Ad) connections were more similar to those observed after injection in PEc than in V6Ad (note the absence of MST connection). Connections of case 18L (one injection in V6Ad partially involving V6Av; another injection in V6Av, partially involving V6Ad; see Table 1) mirrored those with injection in V6Ad and V6Av, respectively.

Table 3 shows that, after caudal SPL injections, labeled areas change according to the area that has been injected. There is a clear top-to-bottom trend in the type of connections, the dorsal area PEc being strongly connected with the inferior parietal and frontal cortex, and the ventral area V6Av with the extrastriate visual areas.

DISCUSSION

General considerations

The aim of this study was to identify the pattern of cortical connections of the visuomotor area V6A (for summary of the functional properties see Galletti et al., 1996, 1999a, 2003). This area has been recently demonstrated to contain two cortical fields, a dorsal one called V6Ad and a ventral one called V6Av (Luppino et al., 2005). The dorsal sector (V6Ad) contains a large proportion of neurons modulated by the movement of the arms. Over the last decade, several papers from our laboratory have described the characteristics of reaching activity in this cortical sector (Galletti et al., 1997; Fattori et al., 2001, 2004, 2005; Marzocchi et al., 2008). We analyzed here the cortical connections of the dorsal sector of V6A by injecting neuronal retrograde tracers within the limits of the cytoarchitectonically recognized area V6Ad. The discussion below refers primarily to the results of five injections in four different hemispheres, all of them located within the limits of V6Ad (see Table 2). Results from injections that crossed into adjacent areas (four cases; see Table 3) are in line with those of cases with "pure" V6Ad injections and will not be further considered. Two cases with injections within the cytoarchitectonic limits of the adjacent fields V6Av and PEc will be used to compare their connections with those of V6Ad (see Table 2). A detailed analysis of the cortical connections of V6Av and PEc is beyond the scope of this paper and will be the aim of future studies.

The present results show that the two cytoarchitectonic fields V6Ad and V6Av have different cortical connections. It has been reported that injections in different parts of the visual field representation of retinotopically organized visual areas produce different cortical connections (see Gattass et al., 1997, for area V2; Palmer and Rosa, 2006, for area MT; Ungerleider et al., 2008, for area V4) and the central visual field is more represented in V6Ad and the periphery in V6Av (see Fig. 2 and Galletti et al., 1996), so it could be that they are two separate areas or two cytoarchitectural fields of the same area. The question of whether V6Ad and V6Av are two separate areas or two cytoarchitectural fields of the same area remains open and will require additional experiments for verification.

V6Ad connections: functional interpretation and comparison with other studies

Figure 13 is an overview of the connections of area V6Ad showing the relative strength of each connection based on the number of labeled cells. V6Ad is connected with areas of the caudal superior and inferior parietal lobules, the intraparietal sulcus, the frontal cortex, and the cortex of the mesial wall of

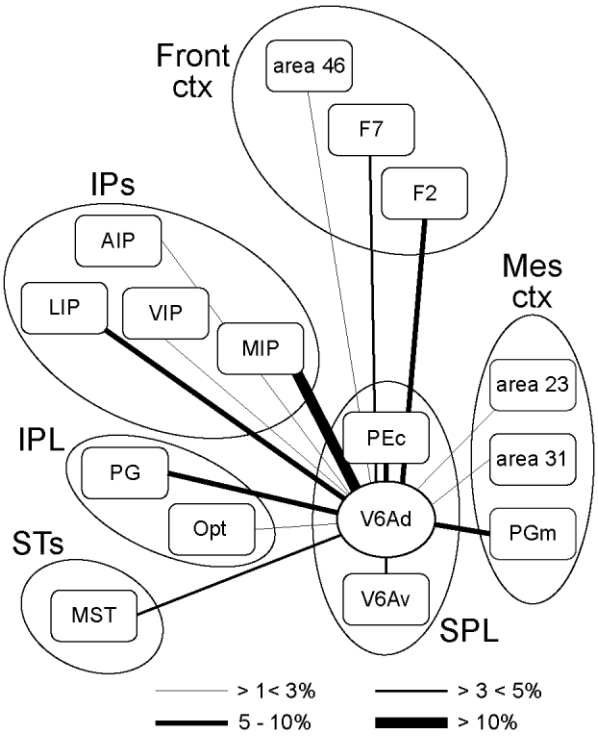

Figure 13.
Summary of V6Ad cortical connections. The flow chart shows the main V6Ad cortical connections. The thickness of the connectional lines is proportional to the strength of connections.

the hemisphere. The strongest connections were with areas MIP and LIP in the intraparietal sulcus, with architectural fields PG in the inferior parietal lobule, F2 (the dorsal premotor area) in the frontal cortex, and PGm in the mesial wall of the hemisphere. In the following, we discuss V6Ad connections by grouping them according to functional criteria.

Connections with areas showing reaching and/or grasping activities. V6Ad receives its major input (about 35% of the total labeled cells) from area MIP. Area MIP contains neurons responsive to passive somatosensory and visual stimulations as well as cells related to active arm-reaching movements (Colby and Duhamel, 1991). Similarly, area V6A shows passive somatosensory (Breveglieri et al., 2002) and visual (Galletti et al., 1999b) cells as well as cells related to active arm-reaching movements (Galletti et al., 1997; Fattori et al., 2001, 2004, 2005). The cortical area called the parietal reach region (PRR; Snyder et al., 1997) mainly overlaps with area MIP (Gail and Andersen, 2006). Area PRR is involved in selecting targets for a reach, planning sequences of reaches, and coordinating eye signals with limb signals and also contains saccade-related activity (Snyder et al., 1997, 2000; Batista et al., 1999; Batista and Andersen, 2001). Similarly, area V6A contains cells active before and during arm-reaching movements (Galletti et al., 1997; Fattori et al., 2001), cells able to code the direction of reaches (Fattori et al., 2005), and cells with saccade-related activity (Kutz et al., 2003). The present data showing a strong connection between MIP and V6Ad, together with the above-reported similarity in functional properties, support the view that the two areas are functionally related. It is likely that these areas form part of a circuit involving reciprocal interaction, in which visual/somatic/motor information is processed before and during the act of reaching. In line with this view, and according to previous results (Johnson et al., 1996; Matelli et al., 1998; Shipp et al., 1998), both areas V6Ad and MIP have a direct, strong connection with area F2, the arm region of the dorsal premotor cortex (Raos et al., 2004). It could be argued that the terms V6Ad and MIP might actually refer to overlapping cortical regions, but the different brain location (see Fig. 1) and the different cytoarchitectonic pattern of the two areas (Luppino et al., 2005) as well as differences in functional properties (see detailed discussion in Galletti et al., 1999b) argue against this hypothesis.

Area PEc represents an important target of V6Ad. The connections of PEc were described by Pandya and Seltzer (1982) and, more recently, by Marconi and coworkers (2001). Both groups reported labeling in the dorsal part of the anterior bank of parietooccipital sulcus, which is putatively in area V6Ad, as well as in areas MIP, PEci, 7m, and MST. In the present work, we observed all these connections when PEc was injected. On the basis of its connectivity (Pandya and Seltzer, 1982) and functional properties (Stein, 1978), PEc was originally considered a somatosensory association area. Because labeled cells were not found in classic somatosensory areas after injections in either areas V6Ad and PEc, we have to admit that somatosensory inputs to V6A and PEc come from other parietal areas, and, among these, area MIP is certainly a good candidate. Recently, visual neurons (Squatrito et al., 2001; Raffi et al., 2002; Breveglieri et al., 2008) as well as hand- and eye-related neurons (Battaglia-Mayer et al., 2001; Ferraina et al., 2001) were found in PEc, suggesting a visuomotor role for this area. This role is well supported by the strong connections of PEc with area V6Ad described here.

Connections of area PGm, which we found strongly connected with V6Ad, were studied by several authors (Pandya and Seltzer, 1982; Cavada and Goldman-Rakic, 1989; Leichnetz, 2001; Parvizi et al., 2006). These studies found connections between PGm and the "parietooccipital area" PO, an area located in the anterior bank of the parietooccipital sulcus (Colby et al., 1988). It has been recently demonstrated that the region originally named PO overlaps partially with the two functionally defined areas V6 and V6A (Galletti et al., 2005; Luppino et al., 2005), although it excludes portions of these same fields (Galletti et al., 1999a; Rosa and Tweedale, 2001). Thus, results of the previous studies describing connections between PGm and PO are not in contrast to our observations, which indicate that both V6Av and V6Ad are connected with PGm, but simply reflect the recent evolution of our knowledge of the subdivisions of this portion of the primate brain. From a functional point of view, cells in area PGm are modulated by eye- and hand-related activity (Ferraina et al., 1997a,b; Thier and Andersen, 1998), like the cells of V6Ad (see Galletti et al., 2003). Unlike V6Ad neurons, however, cells in PGm are reported to be insensitive to visual stimulation (Ferraina et al., 1997a). This functional difference, together with differences in cytoarchitectonic (Luppino et al., 2005) and connectional (Cavada and Goldman-Rakic, 1989) patterns, suggests that PGm and V6Ad are distinct areas.

The strong connections we found between V6Ad and cytoarchitectural field PG, located in the inferior parietal lobule, were also observed in a recent anatomical study (Rozzi et al.,

2006). This study demonstrated that the posterior part of the inferior parietal lobule is directly connected with area V6A, in particular with the portion located in the dorsal sector of the anterior bank of the parietooccipital sulcus. Classical studies on the properties of neurons of Brodmann area 7 in the caudal portion of the inferior parietal lobule (Mountcastle et al., 1975; Lynch et al., 1977; Robinson et al., 1978; Hyvarinen, 1981) reported visual and eye-related activity mixed with passive/active hand/arm movement-related activities. As pointed out by Rozzi and collaborators (2006), the visual, somatosensory, and hand- and arm-related motor inputs that area PG receives are in line with the functional properties of its neurons, reflecting a role in the control of arm movements. As reviewed above, these physiological properties are similar to those found in V6A. Thus, V6Ad–PG connection suggests an exchange of sensory-motor information between these two areas, which likely is functional in the presently unknown role that these areas play in the control of reach-to-grasp movements.

After V6Ad injections, we consistently found a minor connection with area AIP, known to be involved in coding object features and hand movements for grasping objects (Taira et al., 1990; Sakata et al., 1992; Murata et al., 1996, 2000). The connection of V6Ad with area AIP was unexpected in some ways, in that it seems to contrast with the original hypothesis of a strict subdivision between reaching and grasping cortical circuits (see Sakata and Taira, 1994; see Jeannerod et al., 1995). According to this hypothesis, a ventral parietofrontal circuit including AIP and the ventral premotor cortex (area F5) would be involved in the control of grasping, whereas a dorsal parietofrontal circuit including the caudal parietal cortex and the dorsal premotor cortex would be involved in the control of reaching. However, it has recently been demonstrated that lesions of V6A produce misreaching as well as abnormal wrist flexion and rotation in grasping movements (Battaglini et al., 2002). In addition, recent data have shown that V6A contains not only reaching neurons (Fattori et al., 2001, 2005), but also neurons modulated by wrist orientation during prehension of differently oriented objects (Fattori et al., 2004). Finally, Borra and collaborators (2008) found labeling in the dorsal aspect of area V6A, in the cytoarchitectonic field V6Ad, after retrograde and anterograde tracer injections in area AIP. In conclusion, the present data suggest a cross-talk interaction between the dorsal and the ventral parietofrontal networks. Area V6Ad represents a node of this network, being connected with both AIP, specifically devoted to the control of distal arm movements, and F2, containing both reaching- and grasping-related neurons (Caminiti et al., 1991; Boussaoud et al., 1998; Raos et al., 2004; Gregoriou et al., 2005). This supports the view that V6Ad is involved in the control of both reaching and grasping movements (Galletti and Fattori, 2003). This cross-talk, present also in the human brain (Grol et al., 2007), could help in coordinating proximal and distal movements during reach-to-grasp actions.

With regard to the frontal cortex, the present data confirm observations by Matelli and coworkers (1998) of a direct connection between area V6Ad and the ventrorostral part of area F2 (F2vr). This part of area F2 contains neurons coding grip formation and wrist orientation when the animal grasps objects under visual guidance (Raos et al., 2004), as well as visual neurons (Fogassi et al., 1999). Similarly, V6A contains visual-related (Galletti et al., 1999b) and grasp-related (Fattori et al., 2004) neurons. The connections here described between V6Ad and F2vr support the view from the analysis of functional data of an involvement of area V6Ad in the visuomotor coordination of reach-to-grasp movements (Galletti et al., 2003). Similar data have been found for New World monkeys, for which it has been suggested that the dorsoanterior area DA (corresponding to V6A; see Rosa and Tweedale, 2001) has strong connections with the dorsal premotor area, which corresponds to F2 (Burman et al., 2006, 2008). Marconi and collaborators (2001) found, in contrast to the present and previously reported data mentioned above, that after injections in F2 labeled cells were found in area PEc but not in V6A. One possible interpretation is that their injections involved mainly the dorsal sector of F2 (F2d), which, according to Matelli and collaborators (Matelli et al., 1998) as well as the present preliminary results, is primarily connected with PEc.

Marconi and collaborators (2001), in agreement with an earlier report by Matelli and collaborators (1998), described many labeled cells in the ventral part of V6A (putatively in V6Av) after injections in F7. The present data show that also V6Ad is connected with F7. The fact that the rostral premotor cortex, putatively area F7, contains neurons active during reaching activities (Caminiti et al., 1991) as well as visual neurons and cells with eye-related acivities (Boussaoud et al., 1998; Gregoriou et al., 2005) is in agreement with a functional relationship between these two areas.

Colby and coworkers (1988), after injections in area PO, found labeled cells in premotor/prefrontal cortices (putative area F7 and FEF). Because we found such a type of connection when V6Ad but not V6Av was injected, we suggest that PO injection included, at least partially, area V6Ad.

Connections with areas showing oculomotor activity and attentional modulation. V6Ad is connected with area LIP as defined by Seltzer and Pandya (1980) and Blatt and collaborators (1990). Many LIP neurons present saccade-related activity (Blatt et al., 1990; Barash et al., 1991a,b; Colby et al., 1996; Ben Hamed et al., 2001) as well as modulation by visuospatial attention (Bisley and Goldberg, 2006).

We found a minor connection of V6Ad with cytoarchitectural area Opt, which has been proposed to be involved in the shifting of attention in space (Raffi and Siegel, 2005). The caudal part of area 7a (which corresponds to Opt) is considered a site of convergence of eye- and arm-related motor signals in the control of movements in space (Battaglia-Mayer et al., 2005).

V6Ad is also connected with the caudal part of area 23, putatively corresponding to the posterior cingulate cortex of Olson and colleagues (1996). This connection is supported by Morecraft and collaborators (2004), who reported consistent connections of area 23 with the dorsal aspect of "area PO" probably corresponding to V6Ad. Area 23 seems to be involved in visual-spatial processes and spatial attention (Morecraft et al., 2004). V6Ad is also connected with the mesial parietal area 31, whose function is still unclear (see Morecraft et al., 2004).

Finally, the present results show that V6Ad is connected with area 46 in the prefrontal cortex, an area that contains cells sensitive to visual stimulations and saccadic eye movements (Funahashi et al., 1991; Baker et al., 2006) as well as cells related to attention (Ichihara-Takeda and Funahashi,

2007; Watanabe and Funahashi, 2007). Studies in marmoset monkeys demonstrated the same type of connection between the dorsoanterior area (putatively corresponding to V6A) and area 46 (Burman et al., 2006).

The saccade-related activity and the attentional modulation are also present in V6A (Galletti et al., 1996; Kutz et al., 2003). These neuronal properties are well suited for coordinating gaze and attention toward the objects to be grasped (orienting movements), which we suggest is one of the roles in which V6Ad is involved (see Galletti and Fattori, 2003). Common functional properties among interconnected cortical areas support the view of their involvement in a common functional role, in this case that of orienting movements toward the objects to be grasped.

Connections with visual areas. According to the present data, V6Ad is connected with the visual areas V6Av, MST, and VIP but does not receive a direct projection from the extrastriate area V6 (Galletti et al., 1999a). Previous work from our laboratory showed that, after V6 injection, labeled cells were found only in the ventral part of area V6A, putatively in V6Av (Galletti et al., 2001). In the present work, our single injection in V6Av showed that this cortical region receives from V6 and projects to V6Ad. In other terms, visual input could flow from the primary visual cortex to V6 (Galletti et al., 2001), then from V6 to V6Av (Galletti et al., 2001, and present results), then from V6Av to V6Ad (present results), and finally from V6Ad to the dorsal premotor areas F2 and F7 (Matelli et al., 1998; present results). This dorsomedial pathway is one of the shortest circuits through which visual information from the primary visual cortex reaches the motor cortex, along the dorsal visual stream (see Galletti et al., 2004).

The present results show that the visual areas V6Av, MST, and VIP are connected with V6Ad. These three visual areas projecting to V6Ad share a strong sensitivity to the direction of movement of objects in the visual field (Desimone and Ungerleider, 1986; Colby et al., 1993; Galletti et al., 1996). Two of them (V6Av and VIP) also share the presence of the so-called real-position cells, cells whose receptive field remains stable in space during changes in the direction of the gaze (Galletti et al., 1993, 1996; Duhamel et al., 1997). Real-position cells allow encoding of the spatial location of objects present in the visual space (for review see Galletti and Fattori, 2002). We believe that such a type of visual input is very useful for interactions with objects around us during self-movements through the external world and suggest that V6Ad plays an important role in the control of these movements.

CONCLUSIONS

Visual and eye-related activities as well as passive/active arm movement-related activities are very useful in the control of visually guided reach-to-grasp arm movements. Area V6Ad contains neurons with all these functional properties and is most strongly connected with cortical areas showing similar functional properties (Fig. 13). As shown in Figure 13, V6Ad is connected with five main cortical regions: the superior and inferior parietal lobules, the intraparietal sulcus, and the mesial and frontal cortices. In each of these sectors, there is at least one area showing strong connection with V6Ad: PEc, MIP, PG, PGm, and F2, respectively. All these areas, including V6Ad, contain visual, somatosensory, and arm-reaching neurons and have been suggested to be involved in the control of arm-reaching activity. In addition, each of these cortical sectors contains areas showing eye and/or attentional modulations: V6Ad, LIP, Opt, area 23, and 46, respectively. We suggest that the parietofrontal circuit shown in Figure 13 controls both the orienting activities and the visuomotor integrations needed to grasp an object in the extrapersonal space.

AKNOWLEDGMENTS

Prof. Massimo Matelli died in 2003. The authors agreed to remember him in this paper because he participated in the first experiments of this series, even though he did not have the chance to finish the project. The authors thank L. Sabattini, G. Mancinelli, and R. Mambelli for technical assistance.

LITERATURE CITED

Abercrombie M. 1946. Estimation of nuclear population from microtome sections. Anat Rec 94:239–247.

Bach M, Bouis D, Fischer B. 1983. An accurate and linear infrared oculometer. J Neurosci Methods 9:9–14.

Baker JT, Patel GH, Corbetta M, Snyder LH. 2006. Distribution of activity across the monkey cerebral cortical surface, thalamus and midbrain during rapid, visually guided saccades. Cereb Cortex 16:447–459.

Barash S, Bracewell RM, Fogassi L, Gnadt JW, Andersen RA. 1991a. Saccade-related activity in the lateral intraparietal area. 1. Temporal properties—comparison with area 7a. J Neurophysiol 66:1095–1108.

Barash S, Bracewell RM, Fogassi L, Gnadt JW, Andersen RA. 1991b. Saccade-related activity in the lateral intraparietal area. 2. Spatial properties. J Neurophysiol 66:1109–1124.

Barbas H, Pandya DN. 1987. Architecture and frontal cortical connections of the premotor cortex (area 6) in the rhesus monkey. J Comp Neurol 256:211–228.

Batista AP, Andersen RA. 2001. The parietal reach region codes the next planned movement in a sequential reach task. J Neurophysiol 85:539–544.

Batista AP, Buneo CA, Snyder LH, Andersen RA. 1999. Reach plans in eye-centered coordinates. Science 285:257–260.

Battaglia-Mayer A, Ferraina S, Genovesio A, Marconi B, Squatrito S, Molinari M, Lacquaniti F, Caminiti R. 2001. Eye-hand coordination during reaching. II. An analysis of the relationships between visuomanual signals in parietal cortex and parietofrontal association projections. Cereb Cortex 11:528–544.

Battaglia-Mayer A, Mascaro M, Brunamonti E, Caminiti R. 2005. The overrepresentation of contralateral space in parietal cortex: a positive image of directional motor components of neglect? Cereb Cortex 15:514–525 [E-pub 2004 Aug 2018].

Battaglini PP, Muzur A, Galletti C, Skrap M, Brovelli A, Fattori P. 2002. Effects of lesions to area V6A in monkeys. Exp Brain Res 144:419–422.

Ben Hamed S, Duhamel JR, Bremmer F, Graf W. 2001. Representation of the visual field in the lateral intraparietal area of macaque monkeys: a quantitative receptive field analysis. Exp Brain Res 140:127–144.

Bisley JW, Goldberg ME. 2006. Neural correlates of attention and distractibility in the lateral intraparietal area. J Neurophysiol 95:1696–1717.

Blatt GJ, Andersen RA, Stoner GR. 1990. Visual receptive field organization and cortico-cortical connections of the lateral intraparietal area (area LIP) in the macaque. J Comp Neurol 299:421–445.

Borra E, Belmalih A, Calzavara R, Gerbella M, Murata A, Rozzi S, Luppino G. 2008. Cortical connections of the macaque anterior intraparietal (AIP) area. Cereb Cortex 18:1094–1111 [E-pub 2007 Aug 1023].

Boussaoud D, Ungerleider LG, Desimone R. 1990. Pathways for motion analysis: cortical connections of the medial superior temporal and fundus of the superior temporal visual areas in the macaque. J Comp Neurol 296:462–495.

Boussaoud D, Jouffrais C, Bremmer F. 1998. Eye position effects on the neuronal activity of dorsal premotor cortex in the macaque monkey. J Neurophysiol 80:1132–1150.

Breveglieri R, Kutz DF, Fattori P, Gamberini M, Galletti C. 2002. Somatosensory cells in the parieto-occipital area V6A of the macaque. Neuroreport 13:2113–2116.

Breveglieri R, Galletti C, Monaco S, Fattori P. 2008. Visual, somatosensory, and bimodal activities in the macaque parietal area PEc. Cereb Cortex 18:806–816 [E-pub 2007 Jul 2027].

Burman KJ, Palmer SM, Gamberini M, Rosa MG. 2006. Cytoarchitectonic subdivisions of the dorsolateral frontal cortex of the marmoset monkey (*Callithrix jacchus*), and their projections to dorsal visual areas. J Comp Neurol 495:149–172.

Burman KJ, Palmer SM, Gamberini M, Spitzer MW, Rosa MG. 2008. Anatomical and physiological definition of the motor cortex of the marmoset monkey. J Comp Neurol 506:860–876.

Caminiti R, Johnson PB, Galli C, Ferraina S, Burnod Y. 1991. Making arm movements within different parts of space: the premotor and motor cortical representation of a coordinate system for reaching to visual targets. J Neurosci 11:1182–1197.

Cavada C, Goldman-Rakic PS. 1989. Posterior parietal cortex in rhesus monkey: I. Parcellation of areas based on distinctive limbic and sensory corticocortical connections. J Comp Neurol 287:393–421.

Colby CL, Duhamel JR. 1991. Heterogeneity of extrastriate visual areas and multiple parietal areas in the macaque monkey. Neuropsychologia 29:517–537.

Colby CL, Gattass R, Olson CR, Gross CG. 1988. Topographical organization of cortical afferents to extrastriate visual area PO in the macaque: a dual tracer study. J Comp Neurol 269:392–413.

Colby CL, Duhamel JR, Goldberg ME. 1993. Ventral intraparietal area of the macaque: anatomic location and visual response properties. J Neurophysiol 69:902–914.

Colby CL, Duhamel JR, Goldberg ME. 1996. Visual, presaccadic, and cognitive activation of single neurons in monkey lateral intraparietal area. J Neurophysiol 76:2841–2852.

Daniel E, Whitteridge D. 1961. The representation of the visual field on the cerebral cortex in monkeys. J Comp Neurol 248:164–189.

Desimone R, Ungerleider LG. 1986. Multiple visual areas in the caudal superior temporal sulcus of the macaque. J Comp Neurol 248:164–189.

Duhamel JR, Bremmer F, BenHamed S, Graf W. 1997. Spatial invariance of visual receptive fields in parietal cortex neurons. Nature 389:845–848.

Fattori P, Gamberini M, Mussio A, Breveglieri R, Kutz DF, Galletti C. 1999. A visual-to-motor gradient within area V6A of the monkey parieto-occipital cortex. Neurosci Lett 52(Suppl):S22.

Fattori P, Gamberini M, Kutz DF, Galletti C. 2001. "Arm-reaching" neurons in the parietal area V6A of the macaque monkey. Eur J Neurosci 13:2309–2313.

Fattori P, Breveglieri R, Amoroso K, Galletti C. 2004. Evidence for both reaching and grasping activity in the medial parieto-occipital cortex of the macaque. Eur J Neurosci 20:2457–2466.

Fattori P, Kutz DF, Breveglieri R, Marzocchi N, Galletti C. 2005. Spatial tuning of reaching activity in the medial parieto-occipital cortex (area V6A) of macaque monkey. Eur J Neurosci 22:956–972.

Ferraina S, Garasto MR, Battaglia-Mayer A, Ferraresi P, Johnson PB, Lacquaniti F, Caminiti R. 1997a. Visual control of hand-reaching movement: activity in parietal area 7m. Eur J Neurosci 9:1090–1095.

Ferraina S, Johnson PB, Garasto MR, Battaglia-Mayer A, Ercolani L, Bianchi L, Laquaniti F, Caminiti R. 1997b. Combination of hand and gaze signals during reaching: activity in parietal area 7m of the monkey. J Neurophysiol 77:1034–1038.

Ferraina S, Battaglia-Mayer A, Genovesio A, Marconi B, Onorati P, Caminiti R. 2001. Early coding of visuomanual coordination during reaching in parietal area PEc. J Neurophysiol 85:462–467.

Fogassi L, Raos V, Franchi G, Gallese V, Luppino G, Matelli M. 1999. Visual responses in the dorsal premotor area F2 of the macaque monkey. Exp Brain Res 128:194–199.

Funahashi S, Bruce CJ, Goldman-Rakic PS. 1991. Neuronal activity related to saccadic eye movements in the monkey's dorsolateral prefrontal cortex. J Neurophysiol 65:1464–1483.

Gail A, Andersen RA. 2006. Neural dynamics in monkey parietal reach region reflect context-specific sensorimotor transformations. J Neurosci 26:9376–9384.

Galletti C, Fattori P. 2002. Posterior parietal networks encoding visual space. In: Karnath H-O, Milner AD, Vallar G, editors. The cognitive and neural bases of spatial neglect. New York: Oxford University Press. p 59–69.

Galletti C, Fattori P. 2003. Neuronal mechanisms for detection of motion in the field of view. Neuropsychologia 41:1717–1727.

Galletti C, Battaglini PP, Fattori P. 1993. Parietal neurons encoding spatial locations in craniotopic coordinates. Exp Brain Res 96:221–229.

Galletti C, Battaglini PP, Fattori P. 1995. Eye position influence on the parieto-occipital area PO (V6) of the macaque monkey. Eur J Neurosci 7:2486–2501.

Galletti C, Fattori P, Battaglini PP, Shipp S, Zeki S. 1996. Functional demarcation of a border between areas V6 and V6A in the superior parietal gyrus of the macaque monkey. Eur J Neurosci 8:30–52.

Galletti C, Fattori P, Kutz DF, Battaglini PP. 1997. Arm movement-related neurons in the visual area V6A of the macaque superior parietal lobule. Eur J Neurosci 9:410–413.

Galletti C, Fattori P, Gamberini M, Kutz DF. 1999a. The cortical visual area V6: brain location and visual topography. Eur J Neurosci 11:3922–3936.

Galletti C, Fattori P, Kutz DF, Gamberini M. 1999b. Brain location and visual topography of cortical area V6A in the macaque monkey. Eur J Neurosci 11:575–582.

Galletti C, Gamberini M, Kutz DF, Fattori P, Luppino G, Matelli M. 2001. The cortical connections of area V6: an occipito-parietal network processing visual information. Eur J Neurosci 13:1572–1588.

Galletti C, Kutz DF, Gamberini M, Breveglieri R, Fattori P. 2003. Role of the medial parieto-occipital cortex in the control of reaching and grasping movements. Exp Brain Res 153:158–170.

Galletti C, Fattori P, Gamberini M, Kutz DF. 2004. The most direct visual pathway to the frontal cortex. Cortex 40:216–217.

Galletti C, Gamberini M, Kutz DF, Baldinotti I, Fattori P. 2005. The relationship between V6 and PO in macaque extrastriate cortex. Eur J Neurosci 21:959–970.

Gallyas F. 1979. Silver staining of myelin by means of physical development. Neurol Res 1:203–209.

Gattass R, Gross CG. 1981. Visual topography of striate projection zone (MT) in posterior superior temporal sulcus of the macaque. J Neurophysiol 46:621–638.

Gattass R, Gross CG, Sandell JH. 1981. Visual topography of V2 in the macaque. J Comp Neurol 201:519–539.

Gattass R, Sousa APB, Gross CG. 1988. Visuotopic organization and extent of V3 and V4 of the macaque. J Neurosci 8:1831–1845.

Gattass R, Sousa APB, Mishkin M, Ungerleider LG. 1997. Cortical projections of area V2 in the macaque. Cereb Cortex 7:110–129.

Gregoriou GG, Luppino G, Matelli M, Savaki HE. 2005. Frontal cortical areas of the monkey brain engaged in reaching behavior: a ^{14}C-deoxyglucose imaging study. Neuroimage 27:442–464 [E-pub 2005 Apr 2001].

Gregoriou GG, Borra E, Matelli M, Luppino G. 2006. Architectonic organization of the inferior parietal convexity of the macaque monkey. J Comp Neurol 496:422–451.

Grol MJ, Majdandzic J, Stephan KE, Verhagen L, Dijkerman HC, Bekkering H, Verstraten FA, Toni I. 2007. Parieto-frontal connectivity during visually guided grasping. J Neurosci 27:11877–11887.

Guillery RW. 2002. On counting and counting errors. J Comp Neurol 447:1–7.

Hyvarinen J. 1981. Regional distribution of functions in parietal association area 7 of the monkey. Brain Res 206:287–303.

Ichihara-Takeda S, Funahashi S. 2007. Activity of primate orbitofrontal and dorsolateral prefrontal neurons: task-related activity during an oculomotor delayed-response task. Exp Brain Res 181:409–425 [E-pub 2007 Apr 2019].

Jeannerod M, Arbib MA, Rizzolatti G, Sakata H. 1995. Grasping objects: the cortical mechanisms of visuomotor transformation. Trends Neurosci 18:314–320.

Johnson PB, Ferraina S, Bianchi L, Caminiti R. 1996. Cortical networks for visual reaching: physiological and anatomical organization of frontal and parietal lobe arm regions. Cereb Cortex 6:102–119.

Kobayashi Y, Amaral DG. 2000. Macaque monkey retrosplenial cortex: I. Three-dimensional and cytoarchitectonic organization. J Comp Neurol 426:339–365.

Kobayashi Y, Amaral DG. 2003. Macaque monkey retrosplenial cortex: II. Cortical afferents. J Comp Neurol 466:48–79.

Komatsu H, Wurtz RH. 1988. Relation of cortical areas MT and MST to pursuit eye movements. I. Localization and visual properties of neurons. J Neurophysiol 60:580–603.

Kritzer MF, Goldman-Rakic PS. 1995. Intrinsic circuit organization of the major layers and sublayers of the dorsolateral prefrontal cortex in the rhesus monkey. J Comp Neurol 359:131–143.

Kutz DF, Fattori P, Gamberini M, Breveglieri R, Galletti C. 2003. Early- and

late-responding cells to saccadic eye movements in the cortical area V6A of macaque monkey. Exp Brain Res 149:83–95.

Leichnetz GR. 2001. Connections of the medial posterior parietal cortex (area 7m) in the monkey. Anat Rec 263:215–236.

Lewis JW, Van Essen DC. 2000. Mapping of architectonic subdivisions in the macaque monkey, with emphasis on parieto-occipital cortex. J Comp Neurol 428:79–111.

Luppino G, Calzavara R, Rozzi S, Matelli M. 2001. Projections from the superior temporal sulcus to the agranular frontal cortex in the macaque. Eur J Neurosci 14:1035–1040.

Luppino G, Hamed SB, Gamberini M, Matelli M, Galletti C. 2005. Occipital (V6) and parietal (V6A) areas in the anterior wall of the parieto-occipital sulcus of the macaque: a cytoarchitectonic study. Eur J Neurosci 21:3056–3076.

Lynch JC, Mountcastle VB, Talbot WH, Yin CT. 1977. Parietal lobe mechanisms for directed visual attention. J Neurophysiol 40:362–389.

Marconi B, Genovesio A, Battaglia-Mayer A, Ferraina S, Squatrito S, Molinari M, Lacquaniti F, Caminiti R. 2001. Eye-hand coordination during reaching. I. Anatomical relationships between parietal and frontal cortex. Cereb Cortex 11:513–527.

Marzocchi N, Breveglieri R, Galletti C, Fattori P. 2008. Reaching activity in parietal area V6A of macaque: eye influence on arm activity or retinocentric coding of reaching movements? Eur J Neurosci 27:775–789.

Matelli M, Luppino G, Rizzolatti G. 1991. Architecture of superior and mesial area 6 and the adjacent cingulate cortex in the macaque monkey. J Comp Neurol 311:445–462.

Matelli M, Govoni P, Galletti C, Kutz DF, Luppino G. 1998. Superior area 6 afferents from the superior parietal lobule in the macaque monkey. J Comp Neurol 402:327–352.

Maunsell JHR, Van Essen DC. 1983. The connections of the middle temporal visual area (MT) and their relationship to a cortical hierarchy in the macaque monkey. J Neurosci 3:2563–2586.

Mesulam MM. 1982. Principles of horseradish peroxidase neurohistochemistry and their applications for tracing neural pathways-axonal transport, enzime histochemistry and light microscopic analysis. In: Mesulam MM, editor. Tracing neural connections with horseradish peroxidase. New York: John Wiley & Sons. p 1–152.

Morecraft RJ, Cipolloni PB, Stilwell-Morecraft KS, Gedney MT, Pandya DN. 2004. Cytoarchitecture and cortical connections of the posterior cingulate and adjacent somatosensory fields in the rhesus monkey. J Comp Neurol 469:37–69.

Mountcastle VB, Lynch JC, Georgopoulos A, Sakata H, Acuña C. 1975. Posterior parietal association cortex of the monkey: command function for operations within extrapersonal space. J Neurophysiol 38:871–908.

Murata A, Gallese V, Kaseda M, Sakata H. 1996. Parietal neurons related to memory-guided hand manipulation. J Neurophysiol 75:2180–2186.

Murata A, Gallese V, Luppino G, Kaseda M, Sakata H. 2000. Selectivity for the shape, size, and orientation of objects for grasping in neurons of monkey parietal area AIP. J Neurophysiol 83:2580–2601.

Olson CR, Musil SY. 1996. Single neurons in posterior cingulate cortex of behaving macaque: eye movements signals. J Neurophysiol 76:3285–3330.

Palmer SM, Rosa MG. 2006. Quantitative analysis of the corticocortical projections to the middle temporal area in the marmoset monkey: evolutionary and functional implications. Cereb Cortex 16:1361–1375.

Pandya DN, Seltzer B. 1982. Intrinsic connections and architectonics of posterior parietal cortex in the rhesus monkey. J Comp Neurol 204: 196–210.

Parvizi J, Van Hoesen GW, Buckwalter J, Damasio A. 2006. Neural connections of the posteromedial cortex in the macaque. Proc Natl Acad Sci U S A 103:1563–1568.

Passarelli L, Gamberini M, Bakola S, Zucchelli M, Fattori P, Luppino G, Galletti C. 2007a. Cortical connections of the dorso-medial visual areas V6 and V6A in the macaque monkey. Vision Down Under, 7th IBRO Congress of Neuroscience Satellite Meeting on the Eye and Brain, 19–22 July 2007, Palm Cove, Cairns, Australia.

Passarelli L, Gamberini M, Baldinotti I, Fattori P, Luppino G, Matelli M, Galletti C. 2007b. Cortico-cortical connections of dorsal area V6A in the macaque monkey. 7th IBRO Congress of Neuroscience Meeting, 12–17 July 2007, Melbourne, Australia.

Pitzalis S, Galletti C, Huang RS, Patria F, Committeri G, Galati G, Fattori P, Sereno MI. 2006. Wide-field retinotopy defines human cortical visual area v6. J Neurosci 26:7962–7973.

Preuss TM, Goldman-Rakic PS. 1991. Myelo- and cytoarchitecture of the granular frontal cortex and surrounding regions in the strepsirhine primate *Galago* and the anthropoid primate *Macaca*. J Comp Neurol 310:429–474.

Raffi M, Siegel RM. 2005. Functional architecture of spatial attention in the parietal cortex of the behaving monkey. J Neurosci 25:5171–5186.

Raffi M, Squatrito S, Maioli MG. 2002. Neuronal responses to optic flow in the monkey parietal area PEc. Cereb Cortex 12:639–646.

Raos V, Umilta MA, Gallese V, Fogassi L. 2004. Functional properties of grasping-related neurons in the dorsal premotor area F2 of the macaque monkey. J Neurophysiol 92:1990–2002 [E-pub 2004 May 1926].

Robinson DL, Goldberg ME, Stanton GB. 1978. Parietal association cortex in the primate: sensory mechanisms and behavioral modulations. J Neurophysiol 41:910–932.

Rockland KS, Pandya DN. 1979. Laminar origins and terminations of cortical connections of the occipital lobe in the rhesus monkey. Brain Res 179:3–20.

Rosa MG, Tweedale R. 2001. The dorsomedial visual areas in New World and Old World monkeys: homology and function. Eur J Neurosci 13:421–427.

Rosa MGP, Soares JGM, Fiorani M, Gattass R. 1993. Cortical afferents of visual area MT in the cebus monkey: possible homologies between New and Old World monkeys. Vis Neurosci 10:827–855.

Rozzi S, Calzavara R, Belmalih A, Borra E, Gregoriou GG, Matelli M, Luppino G. 2006. Cortical connections of the inferior parietal cortical convexity of the macaque monkey. Cereb Cortex 16:1389–1417.

Sakata H, Taira M. 1994. Parietal control of hand action. Curr Opin Neurobiol 4:847–856.

Sakata H, Taira M, Mine S, Murata A. 1992. The hand-movement-related neurons of the posterior parietal cortex of the monkey: their role in the visual guidance of hand movement. Exp Brain Res Suppl, p 185–198.

Seltzer B, Pandya DN. 1980. Converging visual and somatic sensory cortical input to the intraparietal sulcus of the rhesus monkey. Brain Res 192:339–351.

Shipp S, Blanton M, Zeki S. 1998. A visuo-somatomotor pathway through superior parietal cortex in the macaque monkey: cortical connections of areas V6 and V6A. Eur J Neurosci 10:3171–3193.

Snyder LH, Batista AP, Andersen RA. 1997. Coding of intention in the posterior parietal cortex. Nature 386:167–170.

Snyder LH, Batista AP, Andersen RA. 2000. Saccade-related activity in the parietal reach region. J Neurophysiol 83:1099–1102.

Squatrito S, Raffi M, Maioli MG, Battaglia-Mayer A. 2001. Visual motion responses of neurons in the caudal area pe of macaque monkeys. J Neurosci 21:RC130.

Stein J. 1978. Effects of parietal lobe cooling on manipulative behaviour in the conscious monkey. In: Gordon G, editor. Active touch. New York: Pergamon Press. p 79–90.

Suzuki H, Azuma M. 1976. A glass-insulated "Elgiloy" microelectrode for recording unit activity in chronic monkey experiments. Electroencephalogr Clin Neurophysiol 41:93–95.

Taira M, Mine S, Georgopoulos AP, Murata A, Sakata H. 1990. Parietal cortex neurons of the monkey related to the visual guidance of hand movement. Exp Brain Res 83 1:29–36.

Thier P, Andersen RA. 1998. Electrical microstimulation distinguishes distinct saccade-related areas in the posterior parietal cortex. J Neurophysiol 80:1713–1735.

Ungerleider LG, Galkin TW, Desimone R, Gattass R. 2008. Cortical connections of area V4 in the macaque. Cereb Cortex 18:477–499 [E-pub 2007 Jun 2004].

Van Essen DC. 2002. Windows on the brain: the emerging role of atlases and databases in neuroscience. Curr Opin Neurobiol 12:574–579.

Van Essen DC, Drury HA, Dickson J, Harwell J, Hanlon D, Anderson CH. 2001. An integrated software suite for surface-based analyses of cerebral cortex. J Am Med Inform Assoc 8:443–459.

Vezoli J, Falchier A, Jouve B, Knoblauch K, Young M, Kennedy H. 2004. Quantitative analysis of connectivity in the visual cortex: extracting function from structure. Neuroscientist 10:476–482.

Watanabe K, Funahashi S. 2007. Prefrontal delay-period activity reflects the decision process of a saccade direction during a free-choice ODR task. Cereb Cortex 17(Suppl 1):i88–i100.